ISTITUTO NAZIONALE DI FISICA NUCLEARE

LABORATORI NAZIONALI DI LEGNARO

INFN - LNL

Feasibility Study Report on Alternative $^{99}Mo/^{99m}Tc$ Production Routes using Particle Accelerators at LNL

(2011 version)

Juan Esposito

July 2011

INFN Report
INFN-LNL-235(2011)

Foreword

Nearly 80% of the radioisotopes used in nuclear medicine are currently produced by nuclear reactors. Among these ones, the ^{99m}Tc (6.01 hours half-life), a decay product of ^{99}Mo (65.94 hours half-life) is the most important and widely used one. Every year about 30 million medical procedures, based on ^{99m}Tc-labelled pharmaceuticals for patient diagnostics, are in fact estimated to be performed in the world.

However such a vital radionuclide is mainly supplied by two production facilities only, located in North America, and Europe. Both facilities, which cover about 65% of ^{99}Mo world demand, rely on two nuclear research reactors: the NRU in Chalk River, Ontario (Canada), and the HFR in Petten (The Netherlands). The current ^{99}Mo mass production is, in fact, based upon the isotope separation from fission products by using the Highly Enriched Uranium, Weapon-Grade (HEU-WG) material (^{235}U enrichment > 80%). Such a production is therefore subject to the strict international regulations and control actions against the proliferation of nuclear weapons.

Both reactors have experienced in the recent years (2009-2010) some long scheduled/unscheduled shutdown, almost in the same period, for maintenance/repairs purposes caused by different technical issues. However the problems encountered are mainly referable to their ages (about 40 years operation), being both reactors at the end of their running period. Such an unwanted stop, which has caused a temporary shortage of ^{99}Mo/^{99m}Tc generators on the international market in 2010, has generated new ideas about alternative arrangements, all based on accelerators, as well as making use of non-strategic materials.

Stimulated by medical organizations, the Istituto Nazionale di Fisica Nucleare (INFN) has recently started at Legnaro laboratories (LNL) some preliminary research studies in order to find out alternative ^{99}Mo/^{99m}Tc production routes based upon accelerator-driven neutron sources, as well as investigate the direct molybdenum/technetium production. The main results produced by such a study are here reported. The goal is to get some indications about the contribution that INFN, having expertise both in nuclear physics and particle accelerators could grant to a possible future supply of such radionuclides in Italy, taking into account the new high-performance accelerators which are scheduled to be available in the next years at LNL.

Table of Contents

Summary

Two additional proton accelerators having quite interesting and, at some extent, complementary beam performance are expected to be installed and put into operation at the INFN Legnaro National Laboratories (Padova) in the forthcoming years. The first one is a cyclotron having energy output varying from 40 to 70 MeV and a relatively high beam current up to 500 μA (maximum power 35 kW). The second one is instead a high intensity RFQ (Radio Frequency Quadrupole) type linac, with fixed 5 MeV output energy and beam current ranging from 20 to 50 mA (maximum power 250 kW).

Both accelerators are included as main drivers in two research projects under way at LNL in the last years. The first project, called SPES, aims at constructing a Radioactive Ion Beam's (RIB's) facility dedicated to the nuclear physics research of unstable nuclei, far from stability valley. The second one, called TRASCO-IFMIF is instead focused on the field of applied nuclear physics of the future fusion, as well as Generation-IV fission reactors. The availability of such a driver as an accelerator-driven intense neutron source is also of interest for interdisciplinary medical investigations. Mainly the treatment of advanced stage, resistant tumor kinds by Neutron Capture Therapy (NCT) technique, which has been progressing in the last years. Nevertheless, both accelerators have performances capable of making their use feasible also for the production of some radioisotopes having clinical interest, either by exploiting the direct (p,xn) reaction channel, or by the usual (n,xn) and (n,γ) neutron capture reactions.

A preliminary study, about alternative ^{99}Mo production routes, based upon the aforementioned accelerators has, therefore, been assessed, the main results of which are included in the present report. Being the generator of ^{99m}Tc, a radioactive marker widely used in nuclear medicine for diagnostic use, the production of such a radionuclide is therefore of particular interest. Moreover the ^{99m}Tc direct production route has been taken into account as well, considering the promising results of some recent research performed.

Part I: ^{99}Mo/^{99m}Tc production routes at LNL using proton accelerators

1.1. Background on alternative nuclear reactions for ^{99}Mo/^{99m}Tc production

A simplified ^{99}Mo decay scheme is plotted in Figure 1, showing the intermediate ^{99m}Tc nuclide product in the 87.6% events which, in turn, decays to the ground state ^{99g}Tc and, after quite a long mean time, the ^{99}Ru (stable nuclide) is created. In the remaining 12.4% events the ^{99g}Tc nuclide is instead directly produced form ^{99}Mo decay.

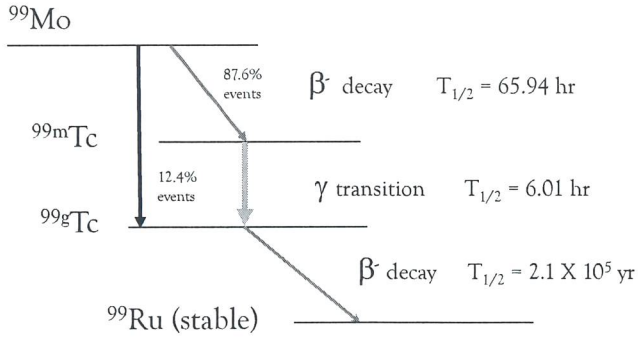

Fig. 1 A simplified ^{99}Mo decay pattern

The main difference between the two nuclides of interest in such a study is that the ^{99m}Tc has a relatively short (about 8.7 h) mean time τ ($T_{1/2}$/ln2), while, on the contrary, ^{99}Mo mean time is about an order of tenth longer (95.2 h), therefore making all the operations required for the preparation of the pharmaceutical products easier.

Granted that all possible ^{99}Mo production routes based upon the isotope separation from uranium or thorium fission products are excluded, the remaining, alternative, ^{99}Mo/^{99m}Tc production methods that would potentially be exploited at LNL, using proton accelerators, entirely rely on the following nuclear reactions enlisted below:

- ^{100}Mo(p,x)^{99}Mo
- ^{98}Mo(n, γ)^{99}Mo
- ^{100}Mo(n,2n)^{99}Mo

} ^{99}Mo production routes

- ^{100}Mo(p,2n)^{99m}Tc
- ^{98}Mo(p,γ) ^{99m}Tc

} ^{99m}Tc production routes

Amongst the five nuclear reactions available, three would directly make use of a proton beam, while the remaining two need an accelerator-driven neutron source, being respectively based on neutron radiative capture and inelastic scattering reactions. Furthermore, two proton-driven reactions taken into consideration would enable the direct ^{99m}Tc production. Such a route, although deemed useful or of

some interest, should however be limited to a local (regional) demand, given the radionuclide decay short mean time. Indeed, the time needed for the fastest chemical processing available since the target End of Bombardment (EOB), up to the final radionuclide-labeled compound ready for the clinical application in the hospitals, is currently reduced to 10÷12 hrs. In such a case the ^{99m}Tc shortening by about a factor of 3÷4 ($N/No=e^{-\Delta t/\tau}$) would occur for decay only. A limiting factor about the quality of the final product obtained with such a route is however the ground state ^{99g}Tc that is both directly produced and generated by parent decay, which content has to be carefully assessed.

Both the isotopes required for the different nuclear reactions concerned are naturally occurring isotopes in the metallic molybdenum in the following atomic abundances:

- ^{100}Mo 9.55%
- ^{98}Mo 24.13%

In order to avoid contaminant radionuclides which can be created through reaction channels opened by the other stable occurring isotopes in the natural molybdenum, namely ^{92}Mo (14.84%), ^{94}Mo (9.25%), ^{95}Mo (15.92%), ^{96}Mo (16.68%) and ^{97}Mo (9.55%), the production estimates for ^{99}Mo/^{99m}Tc nuclides given in the present report will be referred to as 100% enriched ^{98}Mo and ^{100}Mo sample/targets. As reported ahead, in the first experimental investigations performed to assess a production system based upon the aforementioned reactions, highly enriched (97-99%) ^{98,100}Mo materials are in fact usually being considered.

Since samples/targets containing the single isotope only are being considered, confusion is avoided in the concept of *specific activity*, *As*, for the radionuclide of interest produced in the target, so-called in *isotopic carrier* condition. With the term *isotopic carrier*, we mean the total amount of both stable and radioactive atoms of same Z present in the sample. In this respect, some of the definitions found in the regulations extracted from the British Pharmacopoeia (BP) (1993, 1998, 2004), the European Pharmacopoeia (Ph. Eur) (1995, 2005) and U.S. Pharmacopoeia (USP) (1993, 2002) are here reported [1]:

B.P. ('93,'98) version

Specific Activity ***As****: "of a preparation of a radioactive material, is the radioactivity of the radionuclide concerned per unit weight of the element or of the compound concerned".*

USP ('93,'02) version

Specific Activity ***As****: "used to express the activity of a radionuclide per gram of its element"*, that we adopt in this study as reference.

Here is a definition proposed in 2005 by Goeij and Bonardi [1], not in conflict with earlier statements, which may be considered more detailed, although having less practical implementation:

Specific Activity ***As****: "for a given radionuclide, the activity divided by the mass of the sum of all radioactive and stable isotopes isotopic with the element involved. Units: Bq/mol or Bq/kg.*

In all other cases the production effectiveness of the radionuclide concerned will be characterized by means of the *Activity Concentration* $C_{A(t)}$ (i.e. activity/mass substrate (irradiated material)) measured in either Bq/kg or Bq/m^3.

In order to estimate the production level which would be expected using the aforementioned accelerators, a more detailed analysis for each reaction considered, as well as the related excitation function behavior, versus the primary particle energy, is at first given in the following sections.

1.2. ^{99}Mo production routes

1.2.1. Reaction ^{100}Mo(p,x)^{99}Mo

The ^{99}Mo production occurs, in such a case, through two reaction channels: the main one and as decay product of ^{99m,g}Nb when operating at proton beam energies above 10 MeV. The trend of the cumulative cross section measured in different experiments is shown in Figure 2.

- ^{100}Mo(p,pn)^{99}Mo (Q= - 8.3 MeV)
- ^{100}Mo(p,2p) ^{99m}Nb → β$^-$ (15 s), ^{99g}Nb → β$^-$ (2,6 min) } → ^{99}Mo (Q= -11.14 MeV)

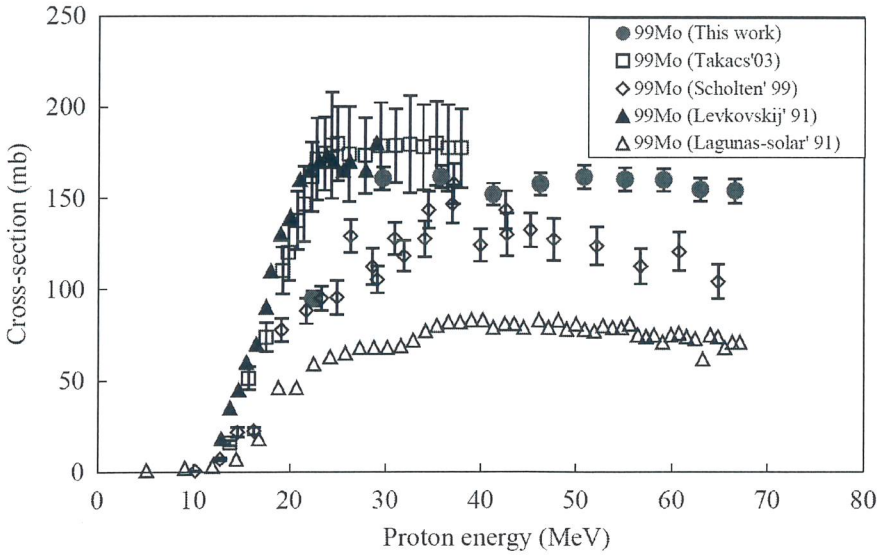

Fig. 2 Excitation function of the ^{100}Mo(p,x)^{99}Mo nuclear reaction [3].

As can be noted, the results of the most recent experimental measurements performed by Uddin et al. [2], are consistent with those by Scholten et al. [3] up to 35-40 MeV protons energy. At higher energies a discrepancy up to 50 mbarn may be seen, while below 20 MeV the data agree well with former measurements made by Takacs et al. [4]. The first cross section measurements reported by Lagunas Solar et al. [5], also given in the plot, are basically lower. It's now generally believed that they have to be considered unreliable.

It should be noted that, additional reaction channels for the production of different Tc, Mo, Nb, Zr, Y isotopes are already opened at protons energy larger than 20 MeV. In the following Figures 3-5 the theoretical excitation functions that had been provided for Mo, Nb and Tc isotopes are shown, based on some nuclear models included in the ALICE code and reported about 10 years ago in the paper by Lambrecht et al. [6].

Although the predictions about the excitation functions for some reaction channels still need to be experimentally validated, e.g. the values for the production of ^{99g}Tc with respect to ^{99m}Tc which contribute to total ^{99}Tc peak production around 1000 mbarn, (see Figure 10 ahead), we are aware that the production of these nuclides is energetically feasible.

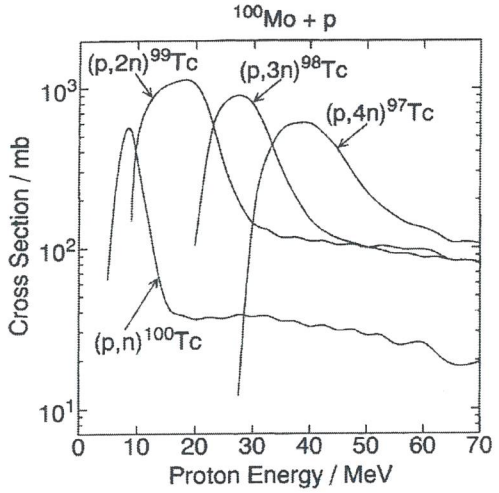

Fig. 3 Excitation function predictions for the production of some Tc nuclides from ^{100}Mo(p,x) reaction [6].

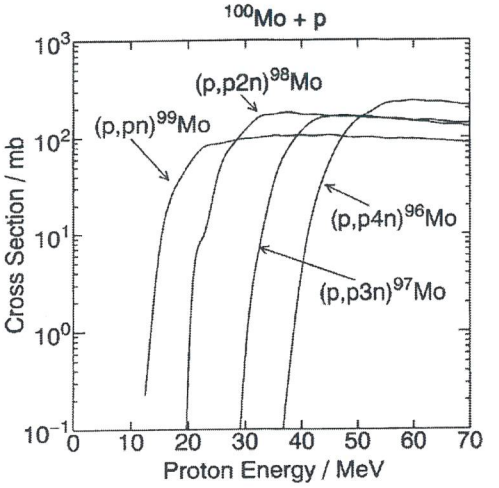

Fig. 4 Excitation function predictions for the production of some Mo nuclides from ^{100}Mo(p,x) reaction [6].

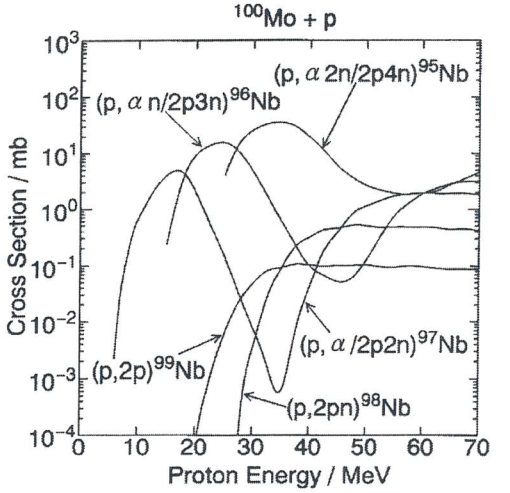

Fig. 5 Excitation function predictions for the production of some Nb nuclides from ^{100}Mo(p,x) reaction [6].

The other Tc isotopes produced have the following decay modes:

- ^{100}Mo(p,4n)^{97}Tc → EC (90d) →^{97}Mo (stable)
- ^{100}Mo(p,3n)^{98}Tc → β$^-$ (4.2E+6 y) →^{98}Ru (stable)
- ^{100}Mo(p,n)^{100}Tc → β$^-$ (15.8 s) →^{100}Ru (stable)

The long-lived radioisotopes thus created, like ^{97}Tc and ^{98}Tc, are however not considered to be a concern in the following chemical processing aimed at the preparation of ^{99}Mo/^{99m}Tc generator. The Ru and Tc elements may in fact be easily separated chemically from Mo for later reuse.

No major problems are reported in literature for the other Mo isotopes produced by other reaction channels. The ^{96}Mo, ^{97}Mo and ^{98}Mo nuclides are, in fact, stable. Since no way to chemically separate such nuclides from ^{99}Mo, the ^{99m}Tc produced would at last be separated chemically from the Mo isotopes mixture in the ^{99}Mo/ ^{99m}Tc generator.

The only issue to be taken into account is the possible reuse of the ^{100}Mo-enriched material (quite expensive). In this case, the original enrichment level available would of course be reduced for a target made by reused material. Additional impurities caused by the reactions on ^{97}Mo and ^{98}Mo created by previous irradiations, would also be produced.

Moreover the production of some Nb nuclides does not involve particular problems. The nuclides created by open reaction channels have the following decay modes:

- ^{100}Mo(p,α2n)^{95}Nb→ β$^-$ (34.98 d) →^{95}Mo (stable)
- ^{100}Mo(p,αn)^{96}Nb→ β$^-$ (23.35 h)→^{96}Mo (stable)
- ^{100}Mo(p,α)^{97}Nb → β$^-$ (72 min) →^{97}Mo (stable)
- ^{100}Mo(p,2pn)^{98}Nb → β$^-$ (51 min) →^{98}Mo (stable)
- ^{100}Mo(p,2p) ^{99m}Nb → β$^-$ (15 s), ^{99g}Nb → β$^-$ (2.6 min) → ^{99}Mo

The use of fully enriched ^{100}Mo targets will never be available in practice; the impurities and the radionuclides by them produced will always be present inside the samples which need to be carefully assessed.

A series of dedicated irradiation tests have already been performed on thick targets in order to assess the ^{99}Mo production level. The integral yields, using 40 MeV proton beams, has been measured to be about 3-4 mCi/μAh [3,4] during the initial irradiation stages ($T_{irr} < \tau/2 = \sim 48$ h). No experimental data is instead available for long irradiation times, close to saturation conditions ($T_{irr} > 4\tau = 380$ h $\cong$ 16 d). Some theoretical estimation from excitation functions performed by Lambrecht et al. [6] suggest that yields around 730 mCi/μA should be obtained at saturation in the range (50–30) MeV. Such a level was basically confirmed by some tests performed later by Scholten et al. [3] at slightly higher protons energy (65 MeV). The estimated yield extrapolated in nearly saturated condition was reported to be about 750 mCi/μA, while integral yields ranging 7.5 mCi/μAh were instead measured at the initial irradiation stages.

1.2.2. Reaction ^{98}Mo(n,γ)^{99}Mo

The ^{99}Mo production is obtained in this case by radiative capture reactions from neutrons having energies either in the thermal range, or within the resonance region. The cross section trend for such a reaction is shown in Figure 6, where the theoretical as well as the experimental measurements from EXFOR database [7] are plotted. In the thermal energy field the value is relatively low, approximately 130 mbarn. Thermal neutron fluence rates of at least (10^{14}–10^{15}) cm^{-2}s^{-1} are therefore needed to get ^{99}Mo mass productions which might be considered feasible following such a route. As known, similar high-level performances may be typically provided by Material Testing Reactors (MTR) facilities only or, alternatively, by accelerator-driven facilities working in the full spallation energy field (n/p ratio ~ 5–10).

An improvement in the overall radiative capture reactions occurs also considering the contribution in the (10 eV-100 keV) energy interval where all the resonances are located, the integral of which is about 6.5 barns. An accelerator-driven neutron source, coupled with a spectrum shifter device, should be set up to provide an epithermal-peaked neutron spectrum instead of a thermal one. A proper spectrum shifter system, using materials with high atomic weights (e.g. lead), having low capture as well as high elastic scattering cross sections, would be the ideal solution. In fact neutrons, losing only a small fraction of energy in each collision, would likelihood be captured crossing the resonance region.

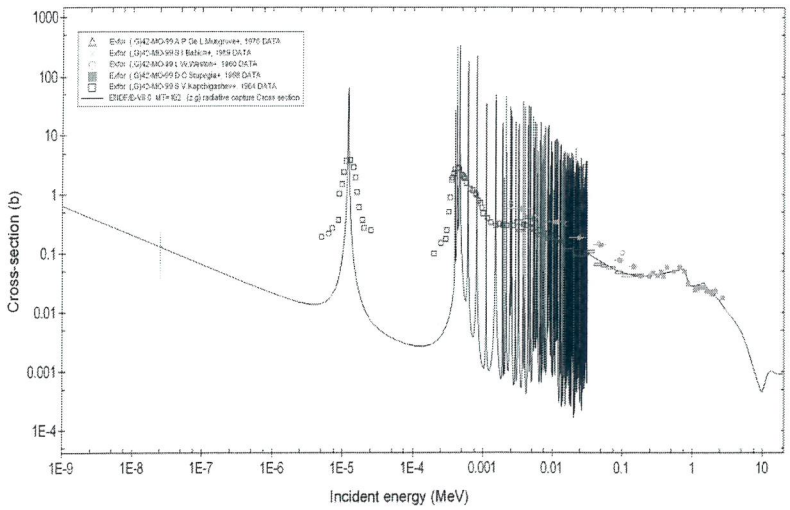

Fig. 6 ^{98}Mo(n,γ)^{99}Mo cross section measurements collection in different experimental campaigns (colored symbols). Theoretical cross section behavior (ENDF-VII) (black line).

Such a behavior, which has been called *Adiabatic Resonance Crossing (ARC)*, although well known in the field of nuclear engineering, was echoed about a decade ago by Carlo Rubbia at CERN [8]. The goal was to study the transmutation effectiveness, through capture/fission reactions, of both Minor Actinides (MA) and Long-Lived Fission Products (LLFP) produced by current (Gen-II) thermal reactors. The system was tested in the TARC experiment [9] (Transmutation by Adiabatic Resonance Crossing), using a spallation neutron source driven by the 3.5 GeV proton beam from PS accelerator at CERN and about 330 tons of lead with 99.99% purity level.

According to the study reported in the enclosed document deposited by Rubbia for the patent request [10], using a neutron source yield of some units in 10^{14} s^{-1}, the specific activity estimated at saturation on natural Mo metal (see point labeled "2" on the plot of Figure 7) is of the order 5-10 mCi/g (~21-42 mCi/g for 100% enrichment). Such a high neutron yield could be achieved at LNL using both the accelerator types under investigation. The thick-target neutron yield from both the Be(p,xn) reaction, recently measured at LNL [11], as well as the Pb,W(p,xn) ones available in literature [12,13], allow to determine that the following neutron source intensities could be achieved by both systems:

- TRASCO RFQ (5 MeV, 30 mA) Be target Sn = $1.05 \cdot 10^{14}$ s^{-1} $\bar{E}n \sim$ 1 MeV
- SPES CYCLOTRON (40 MeV, 500 μA) Be target Sn = $1.40 \cdot 10^{14}$ s^{-1} $\bar{E}n \sim$ 3 MeV
- SPES CYCLOTRON (50 MeV, 500 μA) W target Sn = $2.30 \cdot 10^{14}$ s^{-1} $\bar{E}n \sim$ 4 MeV
- SPES CYCLOTRON (70 MeV, 500 μA) W target Sn = $5.60 \cdot 10^{14}$ s^{-1} $\bar{E}n \sim$ 10 MeV

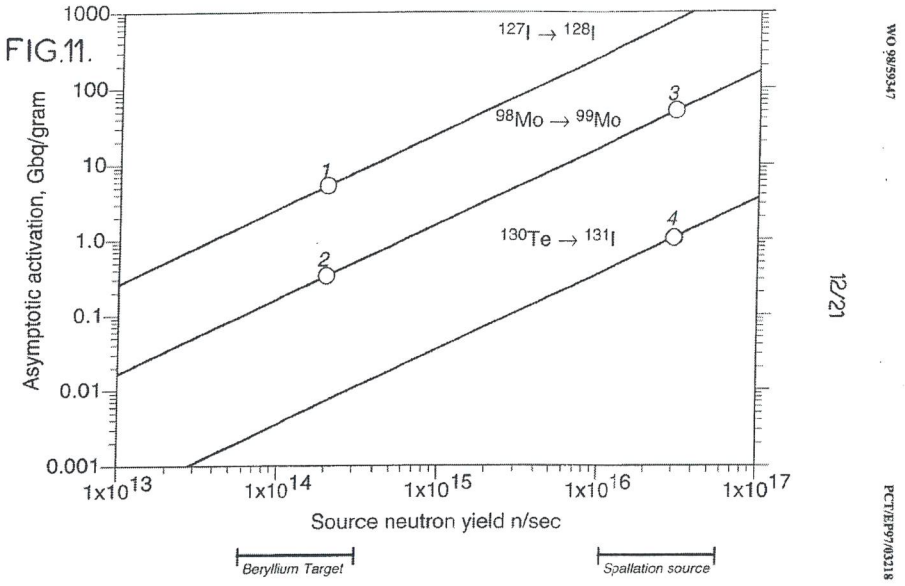

Fig. 7 Specific activity at saturation conditions expected for the $^{98}Mo(n,\gamma)^{99}Mo$ reaction, for natural Mo metal, as a function of the neutron source yield [10].

A small-scale version of the activator system, which exploits the so-called "ARC-method" aimed at the production of radioisotopes for medical use, was realized at Louvain-la-Neuve labs in the early 2000s. A proton cyclotron with maximum output energy of 65 MeV (beam current of a few μA) was used as driver coupled with a thick beryllium target. The results of the experimental tests performed on samples of natural metallic molybdenum are set out in the paper by Froment et al. [14].

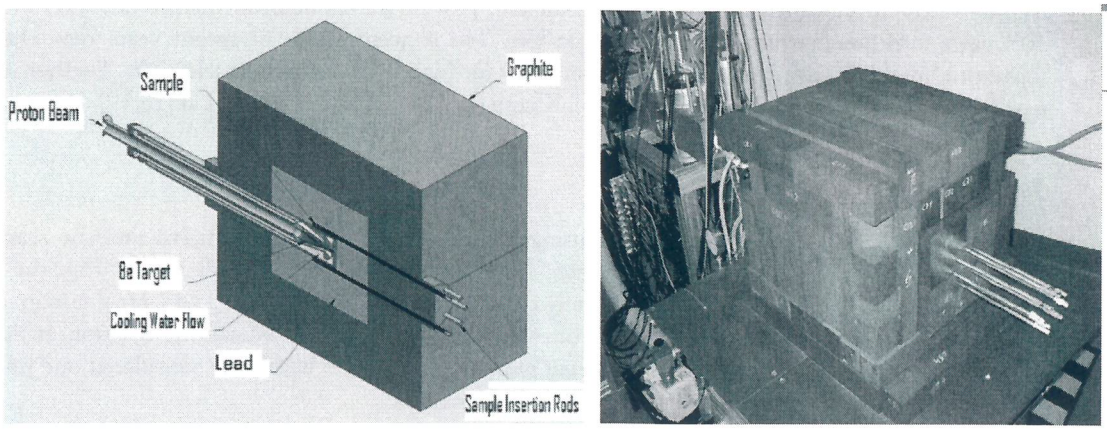

Fig. 8 (left) 3D Sketch of the main components of the neutron activator system. (right) The facility constructed at the JRC Ispra labs for experimental investigations on the production of some radioisotopes for medical interest, including the ^{99}Mo [15].

An even more compact version of the activator system, shown in Figure 8, was recently constructed at the JRC labs in Ispra (Italy) to explore the feasibility of activated nanoparticles (mainly rhenium and indium) to be used in brachytherapy. The system uses a Be-made target, included inside a Pb spectrum shifter volume having (30x30x30) cm^3, large enough to ensure good, although not optimal, ARC effect. The whole system is then surrounded by a RG-graphite reflector, the thickness of which is about 18 cm. The overall sizes are 65x65x65 cm^3.

The Scanditronix MC40 cyclotron therein installed was used, which provides proton beam energies up to 40 MeV and beam currents limited to 60 μA. The radiation tests were instead performed at 36 MeV energy and 35 μA current. Additional details are given in the paper by Abbas et al. [15]. Natural metallic Mo samples were used to estimate the production yields, then rescaled for 100% enriched ^{98}Mo targets.

Provided that an eminently thermal, high fluence rate, irradiation field is available, the main advantage of such a reaction route is the low level of radionuclides contamination which may arise from impurities inside the sample. No other reaction channels, but for the main radiative capture, is in fact opened at relatively low neutron energies. In real cases neutron irradiation facilities driven by mid-size (50-60 MeV) proton accelerators are mainly considered for such projects, which source neutron spectrum mean energy is of the order of 1-5 MeV. Tails extending up to the maximum protons energy are however present and different reaction channels are opened for the production of additional nuclides, including ^{94,95,96}Zr, ^{96,97,98}Nb, ^{90,91}Sr. Many of them decay in a relatively short time (some tens of minutes) in stable nuclides. The only one which might be a potential problem is ^{90}Sr, a well-known beta emitter with $T_{1/2}$=28.8 years. The chemical separation processes, however, should significantly reduce these contaminations from ^{99}Mo.

The main drawback following such a production way is, in any case, the low ^{99}Mo production as shown by the two experimental investigations on natural molybdenum metal targets [14,15]. Because of different irradiation conditions, performed in both experiments at different proton energies and currents, the specific activity estimated per unit beam current would be about 13 μCi/gμA [14] and 18 μCi/gμA [15], quite close to full saturation (7 $T_{1/2}$ = ~4.8 τ, corresponding to 462 hrs = 19.25 d). Such values, once scaled-up for fully-enriched ^{98}Mo samples would become 53.9 μCi/gμA [14] and 74.7 μCi/gμA [15] respectively.

According to such results, a neutron facility driven by 100 μA proton accelerator would achieve specific activities around 5.4 mCi/g at 40 MeV, while about 7.5 mCi/g would be produced at proton beam energies close to 70 MeV. For comparison, ^{99}Mo specific activities about 1-2 Ci/g [4,5] may be achieved when irradiating, under secular equilibrium conditions, ^{98}Mo-enriched samples put inside irradiation

channels close to the core of nuclear reactors able to provide a total neutron fluence rate level of about 10^{13} $cm^{-2}s^{-1}$. Although with such an unfavorable ^{99}Mo concentration, in recent years new chemical separation methods have been developed that allow for high ^{99m}Tc extraction selectivity. Further details, may be seen in the papers by Evans et al. [16], Knapp [17] and Chattopadhyay et al [18,19].

1.2.3. Reaction $^{100}Mo(n,2n)^{99}Mo$

Another option, which may be exploited using fast neutrons, is based on (n,2n) inelastic scattering reactions on ^{100}Mo isotope. The key advantage of this production route mainly comes from the larger cross section value, which keeps approximately constant around 1.3 b in the 12-17 MeV energy range. This value is about tenfold larger than the one for the $^{98}Mo(n,\gamma)$ radiative capture reaction at thermal energies. Aside from the ^{100}Mo elastic scattering reactions (σ_{el} = ~ 2.3 barn), the considered one provides the largest cross section value in the energy region concerned.

Moreover, when a shorter energy window is taken into account (12-14 MeV), the contribution due to the other open reaction channels becomes much smaller (as shown in Figure 9), being the cross sections around 1-2 mbarn. The resulting activity from the other nuclides is therefore markedly limited, making the chemical separation and purification process of the final product easier.

Such a production route has recently been proposed coupled to neutron sources exploiting the $^{3}H(d,n)^{4}He$ (DT) fusion reaction. The main advantage would, in fact, rely on the use of quite simple and compact-size electrostatic accelerator systems working at low energy (100-350 keV), with a high reliability and technology proven. The nuclear fusion reaction $^{3}H(d,n)^{4}He$ has also the advantage to yield an almost isotropic neutron source with a nearly monoenergetic spectrum (14 MeV).

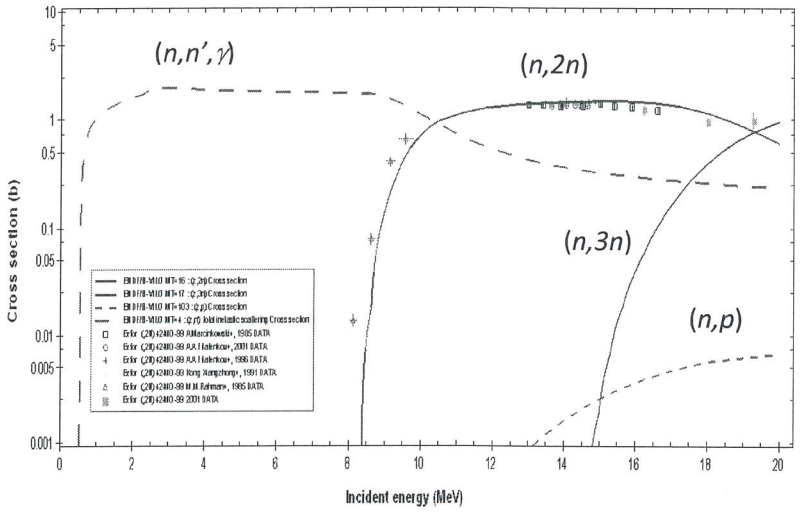

Fig. 9 $^{100}Mo(n,2n)^{99}Mo$ cross section compared to some other ^{100}Mo open reaction channels [7]. All the experimental measurements so far carried out on the (n,2n) reaction are also plotted.

Some production estimates based on such a route have already been reported in the paper by Nagai et. al. [20]. The assumption is to get an irradiation facility able to provide a neutron fluence rate inside the sample volume of the order of 10^{13} $cm^{-2}s^{-1}$ (comparable to that provided by a nuclear reactor). It is reported that after an irradiation time lasting 198 hrs (8.25 d = 2.95 $T_{1/2}$ = 2.04 τ) on 100% enriched ^{100}Mo samples, the specific activity due to ^{99}Mo production would be about 2.1 Ci/g. This is comparable to that obtained by the $^{98}Mo(n,\gamma)$ reaction inside a nuclear reactor under irradiation conditions close to

saturation. By irradiating a ^{100}Mo amount as large as 1 mole (100 g) to be placed around the DT neutron source, a production as high as 210 Ci would be envisaged.

However, the Rotating Target Neutron Source facility (RTNS-II) [21,22] only, built at Lawrence Livermore Labs in the early 1980s as an upgrade of the previous RTNS source, (currently no longer in operation), would have been able to provide such a high neutron fluence rate level inside the sample irradiation volume (a few cm^3). The only high performance neutron source ongoing projects, suitable for radiation damage testing on candidate materials for the next fusion reactors (ITER, DEMO), are the Neutron For Science (NFS), included in the SPIRAL-II facility [23] and the International Fusion Materials Irradiation Facility IFMIF [24]. The total neutron fluence rate expected are of the order of 10^{14} and 10^{15} $cm^{-2}s^{-1}$ respectively.

The DT fusion neutron sources currently available are instead based on the "Sealed Tube" type neutron generator concept in order to limit tritium losses. However the best DT neutron generator which could be available in the near future, actually a modification of the current DD reaction-based source type under development at the Lawrence Livermore National Laboratories (LLNL) in Berkeley [25] to improve its performance, is expected to achieve 10^{13} s^{-1} at maximum. In such a case the best neutron fluence rate estimated would be ~10^{11} $cm^{-2}s^{-1}$ only. Provided the same irradiation time and using the same ^{100}Mo-enriched sample, it is reasonable to estimate a lower ^{99}Mo specific activity produced by a factor 100 (i.e. ~20 mCi/g). By irradiating the same ^{100}Mo mass (1 Mole) a production of about 2 Ci/week might at last be expected.

With the best DT sealed tube generators already available on the market, which neutron yield is 10^{11} s^{-1} only, the predicted ^{99}Mo production would be, at same conditions, a further factor 100 lower, i.e. ~ 0.20 mCi/g. This implies about 20 mCi/week using the same sample mass (1 Mole). We can therefore conclude that the use of this type of neutron source and the expected ^{99}Mo production level using such a reaction route is currently not favorable.

1.3. ^{99m}Tc production routes

1.3.1. Reaction ^{100}Mo(p,2n)^{99m}Tc

A different approach, with respect to the former reactions previously considered, takes into account the direct ^{99m}Tc production without passing through the ^{99}Mo precursor. The radionuclide decay time being short enough ($T_{1/2}$= 6 h), a production system may however still be conceived although limited to regional users (medical centers) surrounding the production plant. Such a reaction route has, in fact, recently been proposed as one of the feasible way to meet the future demand of ^{99m}Tc shortage coming from the reactor-based production [2,3,4,5].

The excitation function, shown in Figure 10, has been repeatedly measured over the past 15 years in different experimental campaigns. In a wide energy range, from 5 up to 70 MeV, there is a single peak, centered around 15 MeV. The peak value, measured in the early 1990s by Levonski et al. [26] and Lagunas Solar et al. [5], repeated by the latter in 1996 (see plot), was estimated at about 300 mbarn. New measurements, repeated about ten years later an reported in the papers by Scholten et al. [3] and Takacs et al. [4], have reduced the value to about 200 mbarn. At proton energies above 30 MeV the cross section quickly drops down to about 15-20 mbarn. Such a reaction route seems therefore to offer potential opportunities to get interesting amounts of ^{99m}Tc using compact accelerators already available (i.e. cyclotrons) with output energies about 20-25 MeV.

Experimental measurements were also carried out in recent years, in order to better determine the impurities produced by other open reaction channels during irradiation. In addiction three tests have been performed (the last two being conducted ten years apart from the first one), which first results are reported in the paper by Scholten et al. [3]. The remaining two are the results of more recent research

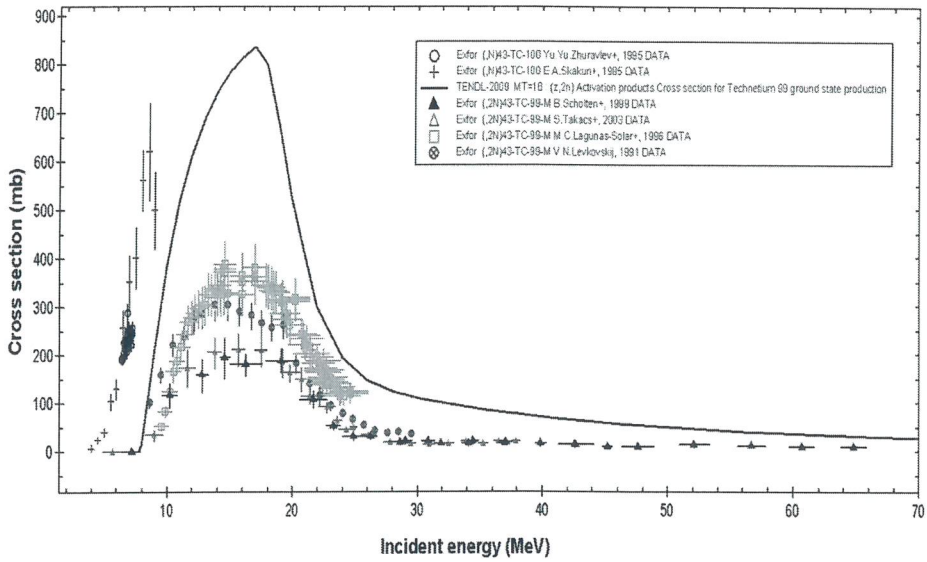

Fig. 10 Composition of experimental excitation functions measured for the $^{100}Mo(p,2n)^{99m}Tc$ reaction. The experimental cross section for the $^{100}Mo(p,n)^{100}Tc$ [3] reaction, as well as the theoretical trend expected for the ground state ^{99g}Tc production [29] are also shown in the plot.

activities, respectively by a Canadian group (Guerin et al. [27]) and an Iranian group (Targholizadeh et al. [28]) both published in 2010.

The first test [3] was performed at two different proton energies: 16 MeV (close to the cross section peak where the maximum of reaction probability occurs) and off-peak at 45 MeV. In both cases thin targets, 97.39% enriched in ^{100}Mo (including 2.58% for ^{98}Mo and other Mo isotopes impurities) were used. The second test [27] was instead run at 17 MeV always on thin ^{100}Mo targets having higher (99.5%) enrichment. The goal of the third test [28] was instead to primarily assess the technological solutions adopted using a relatively high proton beam power (4 kW) and a natural metallic molybdenum thick-target. The estimations for the ^{99m}Tc mass production were then extrapolated considering the thick-target 97.46% enriched in ^{100}Mo (2.54% for ^{98}Mo and other Mo isotopes in traces). Analyses performed through later measurements after sample cooling using gamma spectrometry, have detected the radioisotopes composition enlisted in the following table, as drawn at the End of Bombardment (EOB).

Among all the impurities produced inside the sample, the ones detected having the longest half-life that would remain in the final product because of the same chemical species are the ^{95}Tc ($T_{1/2}$ = 20 h), ^{95m}Tc ($T_{1/2}$ = 60 d), ^{97m}Tc ($T_{1/2}$ = 91.0 d), ^{96}Tc ($T_{1/2}$ = 4.28 d). However, at the end of the preparation process, the contribution given by ^{95}Tc and ^{96}Tc may be considered negligible. Moreover, the values reported by the Canadian group [27] indicate that the impurities are below the limit imposed by the U.S. Pharmacopeia (USP), which maximum is 0.01% in the case of ^{99m}Tc from ^{99}Mo generators. In addition an analysis of residual impurities still remaining after 4 days to completely decay the ^{99m}Tc was also made. The gamma spectrometry revealed no traces of any other type of radioisotope. The results reported by the Iranian group are basically in accordance [28].

It must be pointed out that such a technique cannot detect the production from pure beta-emitters such as the already mentioned ^{90}Sr, which threshold is about 13 MeV [29]. On the other hand, when longer irradiations times approaching saturation ($T_{irr} \geq 3\tau \cong 26$ h) are considered, the contribution due to short-lived impurities will have minor impact than those with longer mean life. In case of proton irradiations using higher energy beams, i.e. 45 MeV (above the resonance peak), the presence of larger radionuclides impurities may be noted. They are originated not only by traces from the other molybdenum isotopes in the sample, but also directly from ^{100}Mo, such as ^{100}Mo (p, 5n)^{96}Tc, whose

target ^{100}Mo	Scholten et al. [3] (1999)	Scholten et al. [3] (1999)	Guerin et al. [27] (2010)	Targholizadeh et al.[28] (2010)
	E=16 MeV T_{irr}= 1hr; relative composition (at EOB) %	E=45 MeV T_{irr}= 1hr; relative composition (at EOB) %	E=17 MeV T_{irr} = 1.5-3 h relative composition (at EOB) %	E=25 MeV T_{irr} = 6.25 h relative composition (at EOB) %
^{99m}Tc	100	100	100	100
^{97m}Tc	<0.026	---	---	---
^{96}Tc	0.005	53	0.0014	0.1785
^{95}Tc	0.016	24.1	0.0010	0.0024
^{95m}Tc	---	5.9	< 0.0003	---
^{94}Tc	0.016	7.2	---	0.0037
^{94m}Tc	0.11	---	---	---
^{93}Tc	---	---	---	0.00092
^{99}Mo	1.34	96.4	traces	traces
^{97}Nb	---	---	traces	---

reaction channel is already open at about 35 MeV. Moreover, the production of the ^{99}Mo precursor is quantitatively equal to that of ^{99m}Tc. In any case, both the ^{100,99}Mo and ^{97}Nb can be separated chemically.

The direct production of ^{99m}Tc is therefore interesting for energies below 25 MeV, so as to minimize the impurities. The thick-target yields resulting from integral calculations, compared to some experimental tests performed at 22 MeV protons energy, is reported by Scholten et al. [3] to be about 11.2 mCi/μAh for the early irradiation stages ($T_{irr} < \tau/2 = \sim 4$ h) and 102.8 mCi/μA at saturation. The first data is basically consistent with the one reported by Takacs et al. [4], which turns out to be ~17 mCi/μAh at the same energy value. When using 40 MeV protons a thick-target yield of 20.6 mCi/μAh [4] has instead been estimated, although irradiations at such energy levels have to be avoided. In the following Figure 11 the comparison between the ^{99m}Tc and ^{99}Mo integral thick-target yields vs. proton energy is finally shown, estimated for both reactions by Scholten et al. [3]. The trend reported in the paper by Takacs et al. [4] is basically similar, but with a slightly better production estimated for ^{99}Mo/^{99m}Tc.

However still an unknown and key issue, is the amount of the ground state, pure β-emitter, ^{99g}Tc which is hard to be determined, being also produced by the same ^{100}Mo(p,2n) reaction [3]. As can be drawn by the plot in Figure 10, the production rate in the 25-10 MeV range for such a long-lived isomer ($T_{1/2}=2.1\cdot10^5$ y), which is useless for diagnostic procedure, is expected to be in excess of a factor 3 than ^{99m}Tc according to the only one theoretical excitation function available from TENDL2009 library [30]. The nuclides ratio $R= N^{99gTc}/N^{99mTc} > 4$ is in fact generally reported to interfere with the functions of some labeled radiopharmaceuticals [31]; a limited number of molecules are considered to be actually attached to image-producing ^{99m}Tc atoms, thus reducing the effectiveness of Tc-based scans. As a consequence, ^{100}Mo samples need to be irradiated for short times, i.e. basically no longer than half-life ($T_{irr} \leq 6$h) so that the N^{99gTc}/N^{99mTc} ratio in the final product may be considered still acceptable, compared to that provided by the current technetium generators. Further studies and experimental campaigns are therefore warmly requested, mainly to validate the ^{99g}Tc excitation functions.

It has to be also noted that some interesting imaging *in-vivo* tests have also been performed by the Canadian group on healthy rats [27], to compare the generator-produced against the cyclotron-produced ^{99m}Tc under quite a short irradiation times (i.e. 1.5-3 hrs) therefore limiting the ^{99g}Tc contamination

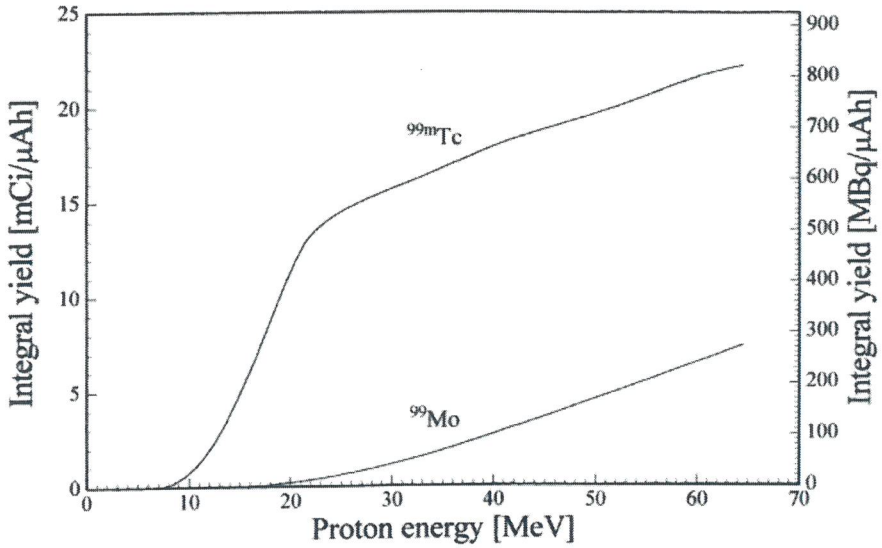

Fig. 11 Integral thick-target yields for ^{99}Mo and ^{99m}Tc nuclides from ^{100}Mo(p,x) reactions estimated from the excitation functions reported by Scholten et al. [3].

level. Three different radiopharmaceutical forms have been prepared: ^{99m}Tc-pertechnetate for thyroid imaging, ^{99m}Tc complex with methylene diphosphate (^{99m}Tc-MDP) for bone scanning, and ^{99m}Tc complex with hexakis-2-methoxyisobutyl isonitrile (^{99m}Tc-MIBI) for heart imaging. Such radiopharmaceuticals cover, in fact, more than ¾ of all routine ^{99m}Tc scans currently used in diagnostic nuclear medicine. The time-radioactivity plots of the three regions of interest around the target organs have been taken during the whole-body planar scintigrams, as well as the tissue uptake selectivity measured in different rats organs after 2.5 hrs injection. The results have clearly shown that the labeling efficiencies, which potentially could be affected by the presence of large quantities of ^{99g}Tc, are instead well above the USP requirements (>90%): 98.4% for ^{99m}Tc-MDP and 98.0% for ^{99m}Tc-MIBI. Further details may be found in the paper by Guerin et al. [27]. Therefore it may be concluded, by these preliminary investigations, that the ground state ^{99}Tc, certainly present in the radiopharmaceuticals, seems to induce a marginal effect on the results from the diagnostic procedures. Biodistribution *in vivo* studies in rats have also been performed with the use of Tc-BRIDA, a neutral lipophilic compound as radio-labeled kit. The radiochemical purity measured in the physiologic saline after the technetium labeling procedure was above 97%. Further details are reported in the paper by Targholizadeh et al. [28].

We should at last mention that the chemical separation process described by Chattopadhyay et al [18.19] can be completed very quickly, just within 1h from EOB, as reported in the paper by Guerin et al. [27]. Quite a short time with respect to that requested for the preparation of the ^{99}Mo/^{99m}Tc generators. In the case of a direct production of ^{99m}Tc it must therefore be assumed that a fully dedicated radiochemical treatment plant for the separation/purification process, up to the production of the radionuclides fulfilling all the required GMP for the prompt utilization, should be available in the same production site of the irradiated samples.

1.3.2. Reaction ^{98}Mo(p,γ)^{99m}Tc

This reaction route (we report it for sake of completeness) provides a contribution to the ^{99m}Tc direct production for protons energy higher than about 10 MeV. However, according to the latest excitation function measured, shown in Figure 12 and reported by Scholten et al. [3], the mean value for proton beam energies ranging from 40 to 70 MeV is in fact of the order of 0.05 mbarn only, quite a low with respect to the other competitor direct reaction channels. Such a contribution can therefore be considered negligible at all.

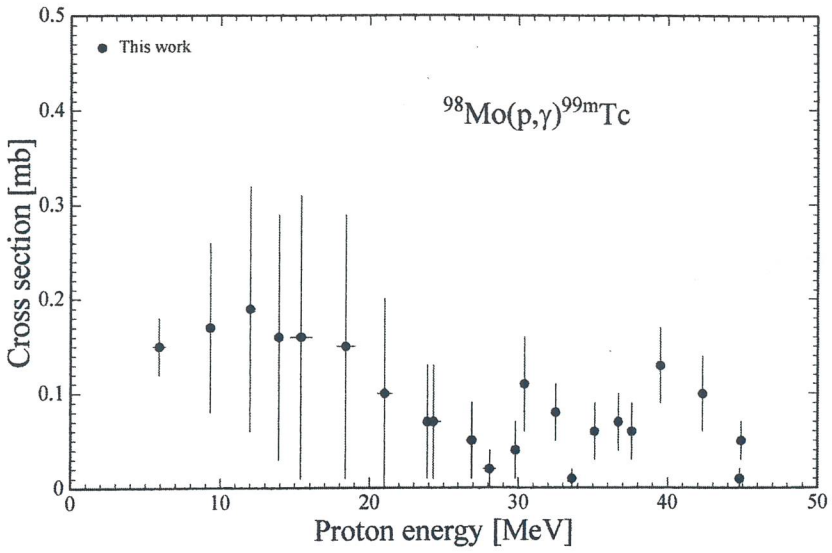

Fig. 12 Excitation function for the reaction ^{100}Mo(p,γ)^{99}Mo [3].

Part II: Preliminary feasibility studies of proton accelerator-driven ^{99}Mo/^{99m}Tc production systems at INFN Legnaro Laboratories

2.1. Preliminary remarks

Given the future availability at Legnaro Labs of proton accelerators whose main performance are mentioned in the summary of this document, the study of some accelerator-driven systems is reported in this section with the aim to produce either the ^{99}Mo parent nuclide or directly the ^{99m}Tc. For any of the production methods proposed, the preliminary analysis results, carried out to estimate the productions expected, are here discussed.

2.2. ^{99}Mo production based on TRASCO RFQ-driven neutron activator

2.2.1. Main features of the activator system proposed

The first irradiation facility concept which has been investigated concerns the ^{99}Mo production through neutron capture reactions on ^{98}Mo, as those discussed in the former part of the document. For such a purpose a proper accelerator-driven activator system, able to provide an epithermal peaked (1 eV-100 keV) neutron spectrum inside the sample holder volume, has been taken into account in order to maximize the ^{98}Mo(n,γ) radiative captures in the resonance energy region. The resulting performance that would be available using the quite intense proton beam driven by the low energy (5 MeV), high-current (30 mA) TRASCO RFQ accelerator [32,33] was firstly assessed because of a similar project currently underway at LNL based on the same driver. The goal is the construction of an accelerator-based intense thermal neutron source dedicated to the BNCT experimental treatments of skin melanoma [34]. Therefore the same Be-based high power neutron converter, which prototype has already been constructed and positively passed almost all the required tests, could be used. Further details are reported in the paper by Esposito et al. [35].

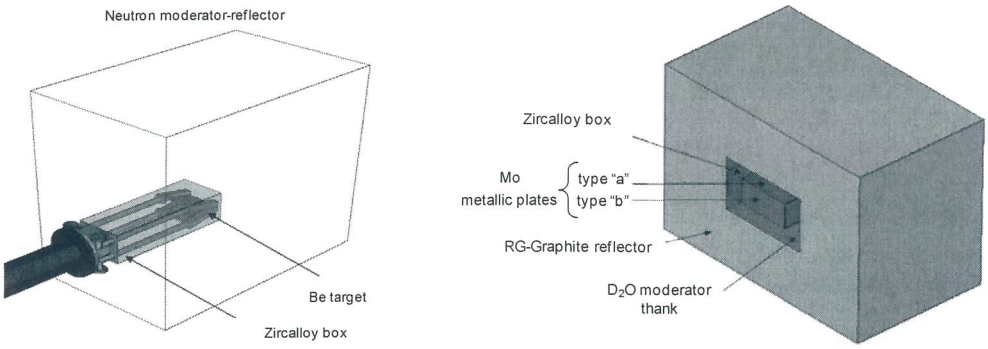

Fig. 13 (left) The neutron activator configuration proposed based on the TRASCO RFQ accelerator and the beryllium neutron converter developed within the BNCT project at LNL [34]. (right) Longitudinal cutaway view showing the activator main components. MCNPX 3D modeling.

The main reason of investigating such a solution is basically due to the relatively low neutron spectrum mean energy provided by Be(p,xn) reactions, being 1.35 MeV only under 5 MeV proton beam (3.2 MeV max energy) [11]. Under these conditions, just a small spectrum shifter (i.e. moderator) volume is therefore needed to slow neutrons, generated by the beryllium target, down to an eminently epithermal neutron source. In such a way neutron captures, as well as losses are minimized during the partial slowing down process. Therefore, based on the experience gained at LNL in the last years, the activator system schematically shown in the following Figure 13 has been modeled for ^{99}Mo production.

The Be neutron converter, located inside a vacuum tight zircalloy holder flanged with the RFQ beam line, is in turn placed inside a D_2O filled tank which acts as main spectrum shifter material. Because of the well-known heavy water neutron *moderating power*, $\xi\Sigma_s$, combined with the excellent *moderating ratio*, $\xi\Sigma_s/\Sigma_a$, neutrons are partly slowed down to the required epithermal energy range, experiencing minimum captures. Moreover, the D_2O box is modeled in such a way as to provide a constant thickness surrounding the zircalloy target holders. In order to assess the best neutron slowing down configuration, a detailed parametric study has been performed for the moderator region only, considering lead as a possible, alternative solution. As shown in the sketch of Figure 14, the benchmark parameter considered for the moderator volume optimization is the thickness "d" around the target.

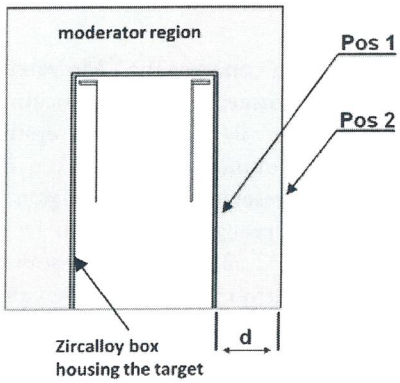

Fig. 14 Cutaway view of moderator region around the Be neutron converter of Figure 13. Possible locations for the ^{98}Mo samples to be irradiated are on the Zircalloy box walls around Be target (Pos 1), or above the moderator side wall (Pos 2).

Different spectrum shifter configurations having increasing volumes have been analyzed in Monte Carlo calculations (MCNPX v2.6a) for both materials. Thicknesses ranging from 5 cm up to 30 cm (with an increasing step of 5 cm), have been taken into account for lead. When D_2O was instead considered, configurations with increasing thickness, from 2 cm up to 10 cm with 2 cm steps, have been simulated. Moreover in all MCNPX calculations performed, the new double differential Be(p,xn) neutron yield spectra at the nominal 5 MeV protons energy, recently measured at LNL [11], have been used to correctly reproduce the neutron emission from the Be target.

Two possible samples positioning have been tested, in order find out the best irradiation conditions assuming to get thin (<1 mm thickness) ^{98}Mo plates: the first one laying down on the zircalloy target holder side wall (called *position 1*), shown in Figure 14, while the second one put on the outer side surface of the moderator volume (called *position 2*). In both positions, in an empty volumetric region of (30x15x0.1) cm^3, the volume-averaged neutron fluence has been calculated in the three main energy ranges: thermal (E_n < 1eV), epithermal (1 eV <E_n< 100 keV) of interest to test the ^{98}Mo neutron capture in the resonance region and, finally, the fast energy region (E_n > 100 keV). Figure 15 shows the resulting neutron fluence in the epithermal range (normalized per unit neutron source) calculated for the two irradiation positions vs. the moderator thickness, for both spectrum shifter configurations and without the contribution of a neutron reflector.

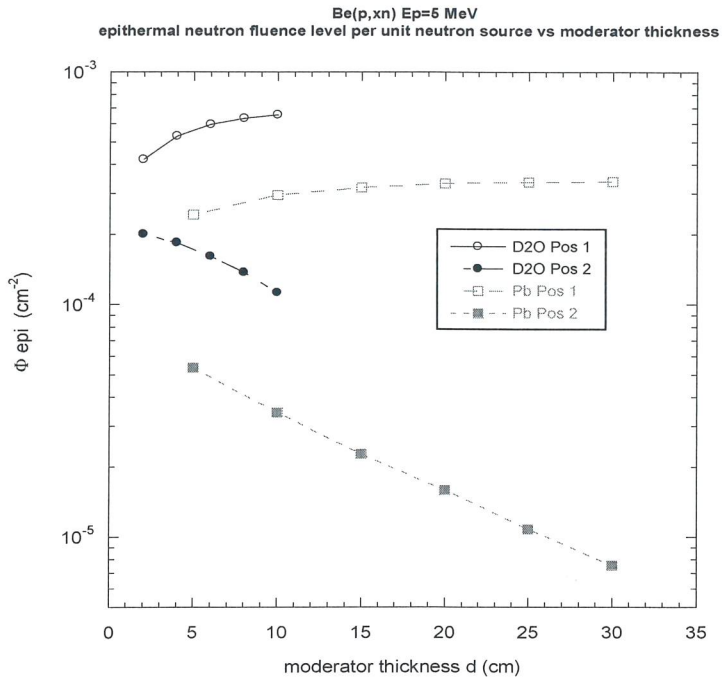

Fig. 15 Neutron fluence calculated in the 1 eV<E_n<100 keV energy range for both irradiation positions shown in Figure 14, versus the D_2O and Pb moderator thickness arranged around target.

As may be noted, the best performance may be achieved using both moderator materials when samples are located at the *position 1*. In particular, the maximum epithermal fluence level is reached using D_2O as moderator having a thickness of just 10 cm surrounding the zircalloy box. When using Pb as spectrum shifter material the epithermal fluence level is instead twice lower, whose saturation is achieved when the material thickness approaches 30 cm.

The source neutron spectrum shifting effectiveness towards the epithermal energy range however is not the unique parameter which is required by an activator system. In order to have a net increase of the neutron fluence level in the epithermal energy range, a good *spectral selectivity (i.e. spectral ratio)* is indeed needed as well, with minimum neutron losses and limited neutron slowing down towards lower energy groups. In the next plot shown in Figure 16, the spectral selectivity in the epithermal energy range are plotted for both moderator materials against the moderator thickness, calculated in the two aforementioned irradiation positions.

The best performance in such a case is achieved still using D_2O as spectrum shifter material having just 8 cm thickness, although located at the moderator outer wall (*position 2*). However, it has to be noted that

the epithermal-to-total spectral ratio would be just 30% better than the corresponding value calculated at the *position 1*.

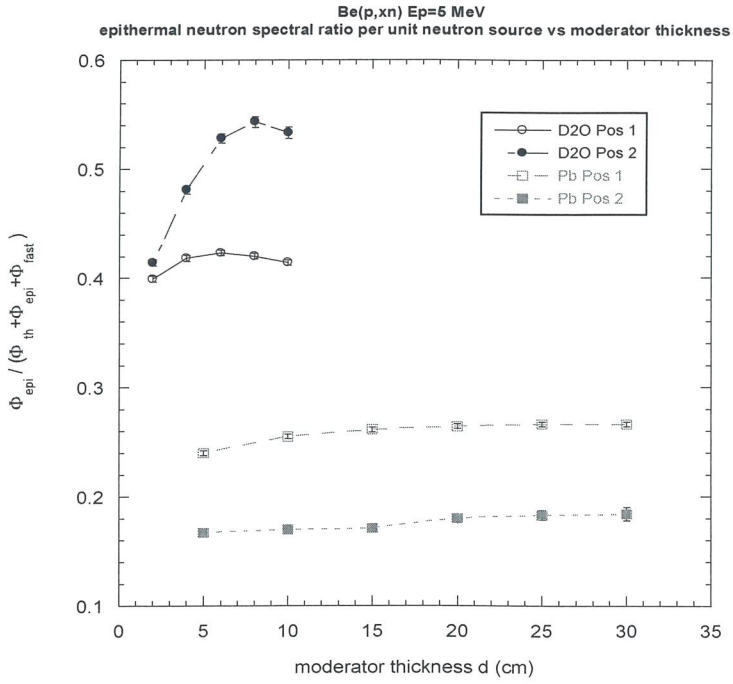

Fig. 16 Neutron spectra selectivity in the epithermal range (spectral ratio), versus D_2O and Pb moderator thickness around the target, corresponding to the irradiation positions shown in Figure 14.

On the other hand the neutron fluence level which would be available at the irradiation *position 2* (see Figure 15) drops down by a factor 4.6 compared to the estimated value at the *position 1*. The best compromise for the activator configuration is therefore based on a spectrum shifter stage in D_2O having about 10 cm thickness.

The next step for the activator system configuration is the assessment of the best reflector configuration. In this case, given the neutron source spectrum relatively low mean energy, one of the proper materials having good albedo properties, low cost, and relatively easy procurement, is Reactor Grade (RG)-graphite [34]. The final modeling proposed is shown in Figure 13; the D_2O spectrum shifter volume required is about 70 dm^3, surrounded by a RG-graphite reflector. The 100% enriched ^{98}Mo thin plate samples are supposed to lay down on the Zircalloy box outer side walls around the neutron converter (*position 1*). Those referred to as "type a " (located on the top and bottom surfaces) have sizes (30x26.4x0.1) cm^3, while those indicated as "type b" (on right-left walls) have size (30x15x0.1) cm^3.

In order to find out the optimal reflector thickness an additional parametric study has been performed; the volume-averaged ^{99}Mo production rate has been calculated for both sample types, corresponding to that achieved at saturation. The results are shown in the following Figure 17, normalized per unit volume and per source neutron, versus the RG-graphite thickness surrounding the moderator. For sake of symmetry, a single ^{99}Mo production trend is shown in plot for both sample types "a" and "b". The statistical calculation errors are within 0.5%.

A different ^{99}Mo production may be noted in both cases, as expected, caused by slightly different neutron spectra at both sample positions. Indeed, neutrons passing through "type a" ^{98}Mo samples, which are located above and below the two halves making the V-shape like Be-target (see Fig. 13), experience a higher probability of being further slowed down from the Be target itself, thus improving

the radiative capture process. The ^{98}Mo "type b" samples are instead mainly crossed by neutrons without being further moderated by the Be target.

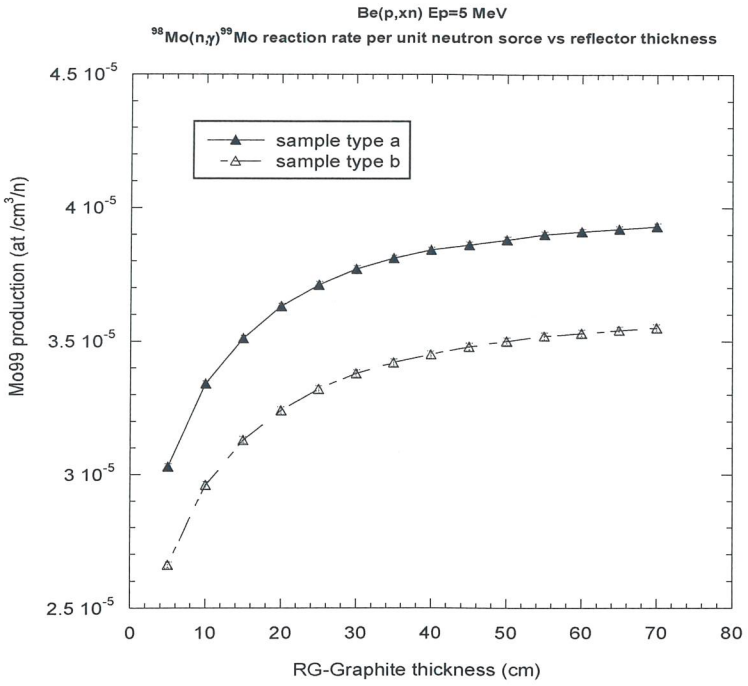

Fig. 17 Normalized ^{99}Mo production expected by ^{98}Mo(n,γ) reaction using 100% enrichment samples, with the proposed TRASCO-RFQ driven activator system and the Be neutron converter developed, versus the RG-Graphite thickness.

A slightly harder spectrum, mainly due to geometry constraints, is therefore available in this position causing minor capture events. The data show an improvement of about 80% in the ^{98}Mo(n,γ) production, reaching an almost asymptotic condition, when the RG-graphite reflector having at least 70 cm thickness is used. Provided that the ^{99}Mo production out of total due to the last 30 cm reflector thickness is about 2% only, the minimum required RG-graphite thickness is 40 cm. The final estimated overall sizes for the activator system proposed are (L, W, H) (134x126x117) cm^3.

The normalized neutron fluence spectra, calculated for the "type a" position where ^{98}Mo samples are irradiated, are shown in the next Figure 18. The spectra plotted are referred to both configurations in which either the bare target only (without D_2O moderator and the 40 cm thickness RG-reflector), or the complete system are considered. The resulting neutron spectrum in the irradiation position may therefore be accounted as the optimal one, because of a neutron fluence trend actually flat in the 1 eV-100 keV energy range, which integral is $5.5 \cdot 10^{-4}$ cm^{-2}. Provided that the TRASCO RFQ + Be target system is expected to generate, at the operating working conditions (see § 1.2.2), a neutron source intensity around $1.05 \cdot 10^{14}$ s^{-1}, an epithermal neutron fluence rate level $\Phi_{epi} \sim 6.0 \cdot 10^{10}$ cm^{-2}s^{-1} would at last be available in the aforementioned sample position.

In order to assess the soundness of the proposed activator system based on TRASCO RFQ accelerator, a comparison has also been performed with the similar system developed at the JRC Ispra lab [15] mentioned earlier, based on a cyclotron-driven 40 MeV proton beam (see § 1.2.2), which spectral features are shown in Figure 19.

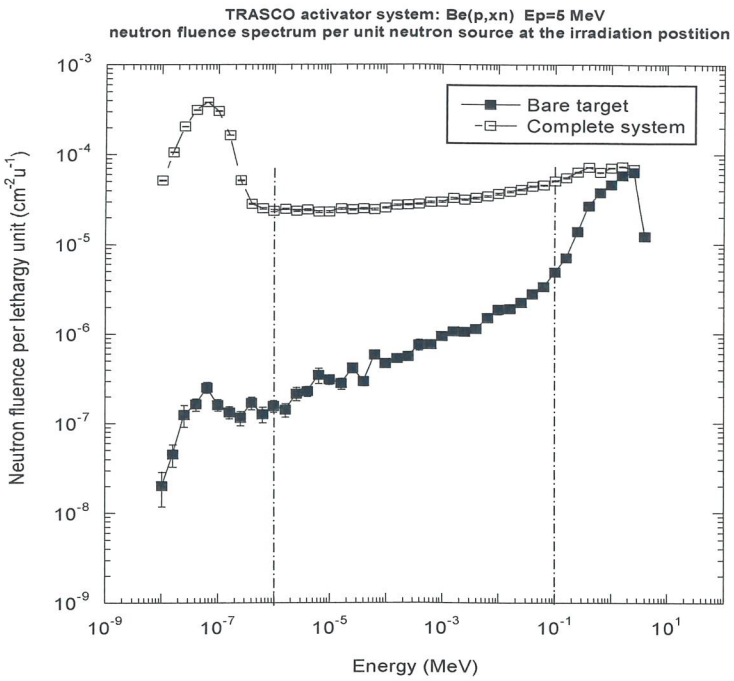

Fig. 18 Normalized neutron fluence spectra comparison which would be available at the "type a" irradiation position with the proposed TRASCO RFQ driven activator system. The neutron spectrum yielded by the bare Be target only (full square plot), as well as the one considering the complete irradiation configuration (void square plot) are shown.

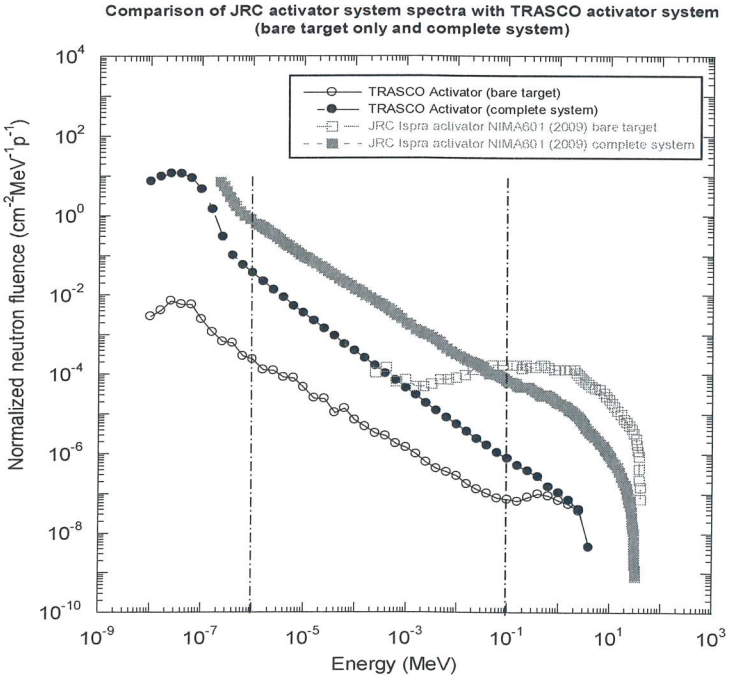

Fig. 19 Neutron fluence spectra comparison at the sample irradiation positions, normalized per unit energy and unit proton hitting the target, between the JRC activator system (red plots) [15] and the proposed system based on TRASCO RFQ accelerator (black plots). Neutron spectra which would be available concerning the bare target only as well as and the complete systems are also shown.

The analysis of normalized neutron spectra for the complete system shows a similar trend in both cases. Such a behavior means that the activator system proposed, based on TRASCO RFQ driver, is able to provide a spectral quality level in the epithermal energy range as high as the JRC cyclotron-driven activator system, with an even better quality performance at lower (thermal) neutron energies.

By integrating the spectra plots between the 1 eV - 100 keV, the resulting normalized neutron fluence level for the JRC activator is better than the proposed one by about a factor 70. Such a difference may however be basically accounted for the improved n/p efficiency from Be(p,xn) reactions at higher proton energies. At E_p = 40 MeV the neutron yield is $2.09 \cdot 10^{11}$ $s^{-1} \cdot \mu A^{-1}$ (see Table 1 ref. [15]) compared to $3.5 \cdot 10^{9}$ $s^{-1} \cdot \mu A^{-1}$ [11] available at E_p= 5 MeV that is, in fact, lower by about a factor 60. The less efficient neutron production at low proton energies is, however, largely recovered by the quite superior TRASCO RFQ accelerated beam current.

2.2.2. Expected ^{99}Mo production with TRASCO RFQ-driven neutron activator

On the basis of the preliminary modeling stage for the proposed TRASCO RFQ driven neutron activator system, the ^{99}Mo production by radiative capture reactions may, at last, be assessed with a good accuracy. The main reference parameters and the calculated values aimed at the final estimations of ^{99}Mo specific activity expected both after the first 24 hrs irradiation and at saturation, are enlisted in the following table.

Activator System based on TRASCO RFQ + Be target			
TRASCO RFQ output energy	Ep	5	MeV
Proton beam current	Ip	30	mA
Beam power on target	P	150	kW
Neutron converter material		Be	
Estimated TOTAL neutron source	$S_{n\,tot}$	$1.05 \cdot 10^{14}$	s^{-1}
Epithermal neutron fluence rate (1eV-100 keV) at sample position	$\Phi_{n\,epi}$	$5.8 \cdot 10^{10}$	$cm^{-2}\,s^{-1}$
TOTAL neutron fluence rate at sample position	Φ_{tot}	$3.05 \cdot 10^{11}$	$cm^{-2}\,s^{-1}$
Irradiated sample: ^{98}Mo (enrichment)	%	100	
Production route	Mo98(n,γ)Mo99		
Estimated TOTAL Reaction Rate (RR) inside sample		$4.03 \cdot 10^{9}$	$cm^{-3}\,s^{-1}$
RR fraction due to epithermal neutrons (1eV-100 keV)	%	88.5	
^{99}Mo Specific Activity at saturation ($T_{irr} \cong 5\,\tau \cong 20$ days)	As*	10.60	mCi/g
^{99}Mo Specific activity (first 24 hrs)	As	2.36	mCi/g
^{98}Mo bulk mass requested for 1 Ci ^{99}Mo production (first 24 hrs)	m	423	g
Additional open reaction channels	Zr95 only → Mo95 stable		

Starting from the data obtained by MCNPX simulations, the *effective* microscopic cross section σ_{eff} in the resonance region, which must be used in simplified calculations to correctly weight the ^{99}Mo production in the epithermal range, may now be estimated. The MCNPX code in fact, using the continuous-energy evaluated cross sections provided by the primary sources of nuclear data libraries (e.g. ENDF, ENDL etc), takes into account the resonance behavior for the ^{98}Mo(n,γ) radiative capture reaction in such an energy range. The ^{99}Mo production rate calculated inside the sample region (nuclides created per unit time and volume) in the 1 eV-100 keV range (see table) is therefore:

$$Y^{99Mo} = \int_{1eV}^{100\,keV} n_{98_{Mo}}\,\sigma(E)\Phi(E)dE = 4.03 \cdot 10^{9} \cdot 0.885 = 3.57 \cdot 10^{9}\mathrm{cm}^{-3}\mathrm{s}^{-1}$$

with $n_{98_{Mo}} = 6.45 \cdot 10^{22}\ cm^{-3}$ ^{98}Mo (~ ^{nat}Mo) atom density

since the neutron flux-weighted microscopic cross section in the epithermal energy range is, by definition:

$$\sigma_{epi\,eff} = \frac{\int_{1eV}^{100\,keV} \sigma(E) \cdot \Phi(E)dE}{\int_{1eV}^{100\,keV} \Phi(E) \cdot dE}$$

the following relation may be always formally reported (the reaction rate invariance):

$$Y^{99Mo} = \int_{1eV}^{100\,keV} n_{98_{Mo}}\,\sigma(E)\Phi(E)dE = n_{98_{Mo}}\sigma_{epi\,eff} \int_{1eV}^{100\,keV} \Phi(E)\,dE$$

where

$$\Phi_{\mathrm{epi}} = \int_{1eV}^{100\,keV} \Phi(E)\,dE$$

The flux-weighted ^{98}Mo cross section mean value in the epithermal energy range is, at last, given by the next relation:

$$\sigma_{epi\,eff} = \frac{Y^{99Mo}}{n_{98_{Mo}}\Phi_{epi}} = \frac{3.57 \cdot 10^{9}\ cm^{-3}s^{-1}}{6.45 \cdot 10^{22}\ cm^{-3} \cdot 5.8 \cdot 10^{10}\ cm^{-2}s^{-1}}$$

$$\sigma_{epi\,eff} = 0.095 \cdot 10^{-23}\ cm^{2} \approx 0.95\ barn$$

Such a value is therefore well below the 6.5 barn accounting for the resonance integral, which is usually mentioned to indicate the effectiveness for ^{98}Mo(n,γ) radiative capture reaction by the so-called "ARC method" (see § 1.2.2).

Similarly, the flux-weighted$\sigma_{epi\,eff}$, value, estimated over the whole neutron energy interval, is as low as ~ 0.20 barn.

2.3. ^{99}Mo production based on SPES cyclotron-driven neutron activator

2.3.1. Main features of the activator system proposed

The ^{99}Mo production by means of neutron capture reactions on ^{98}Mo-enriched samples could be also achieved at LNL taking into account an activator system driven by the high performance (40-70 MeV, 500 μA max beam current), proton cyclotron of the future SPES project [36]. A better neutron yielding efficiency n/p would, in such a case, be available for the neutron source generation, working at higher proton energies than that provided by TRASCO RFQ. The activator system conceived, which modeling is basically a scaled-up version of the one already developed both at the JRC Ispra site [15] (see § 1.2.2) and at Louvain-la-Neuve laboratory [14] for experimental studies, is schematically shown in Figure 20.

In order to get some indications about the ^{99}Mo production level expected by such a system, the modeling has been performed considering, as reference, an intermediate level among the wide range of cyclotron output energies. Moreover, unlike the two aforementioned systems constructed, in the present study a tungsten neutron converter has been taken into account instead of a beryllium one, because of two basic issues. The first one consisting in the improved neutron yielding efficiency n/p generally provided by higher-Z materials (approximately 20-50% better in the 40-70 MeV range); the second one the more favorable lower mean energy spectrum from source neutrons, which are moreover yielded in a roughly isotropic way.

Detailed experimental data on neutron yield spectra for W(p,xn) reaction are already available at E_p=50 MeV [13] and shown in Figure 21. It was thus decided to adopt this energy level as reference for the entire protons energy range. In such a way both the proton transport and the nuclear interaction processes inside the target bulk material (which are computing time consuming) have been skipped in MCNPX calculations, by directly simulating the neutron source distribution. Moreover, the current nuclear evaporation models included in the more widely used transport codes, are known to be unreliable enough. For proton energies still far from the full spallation region, differences of a factor 2-4 in the neutron yield calculation are currently given, compared to reference experimental data.

The neutron converter modeled, similar to the one developed for the neutron activator system at the JRC Ispra site, is of conical shape and light-water cooled. It is located within a Pb-based spectrum shifter volume acting as neutron buffer. Because of lead quite a low moderating power for neutrons, being gradually slowed down due to the "ARC effect" mentioned earlier (see § 1.2.2), they are able to "scan" the molybdenum cross section resonances with an enhanced neutron capture occurring probability.

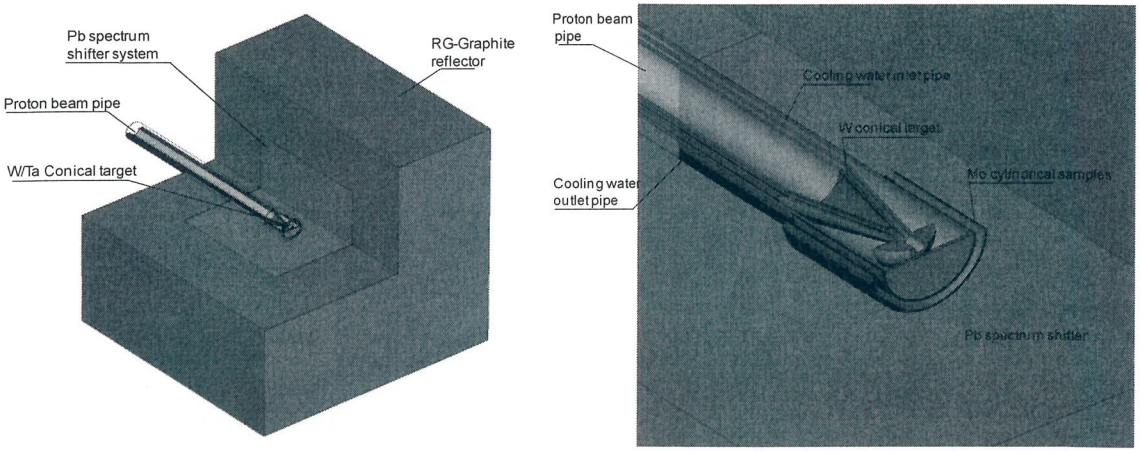

Fig. 20 (left) A simplified sketch of the proposed neutron activator system based on the SPES cyclotron-driven proton accelerator: main layout components. (right) Detail of the target zone housing the samples compartment (considered as Mo cylindrical shells) to be irradiated. MCNPX 3D modeling.

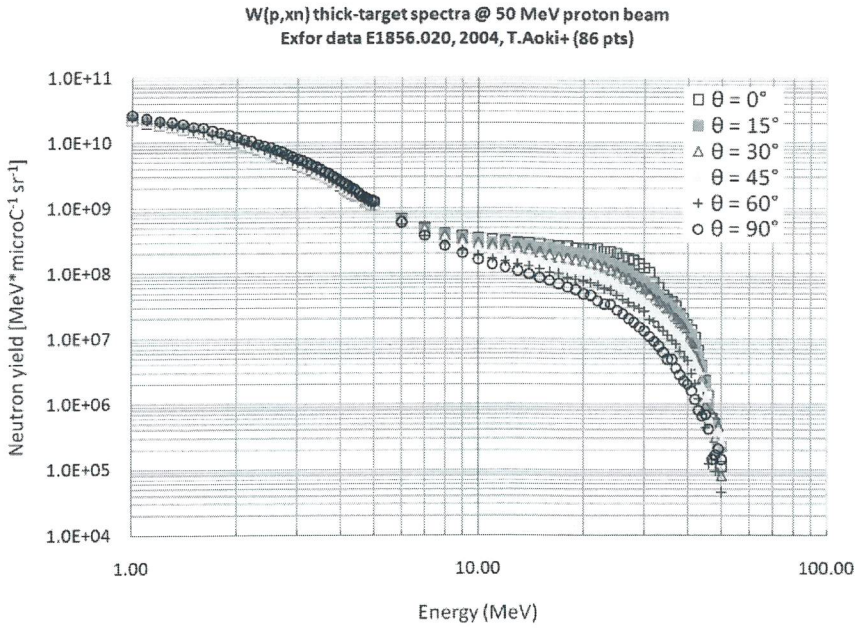

Fig. 21 Experimental measurements of angle-dependent thick-target neutron yield spectra for W(p,xn) reaction at Ep=50 MeV. Further details may be found in the paper by Aoki et al. [13].

The use of light moderator materials like D_2O, as done for the TRASCO RFQ-based activator system modeling, would not be the optimal solution in this case. The average lethargy increment during the neutron slowing down process using heavy water as moderator ($\overline{\xi_{D_2O}} = 0.508$) is, in fact, about 50 times larger than lead ($\overline{\xi_{Pb}} = 0.0095$). This implies that neutrons lose about 40% of their energy after each collision, compared to about 1% only in case of lead. The source spectrum mean energy being about 4 MeV (10% neutrons out of total, have energy higher than 5 MeV), neutrons would then experience jumps in energy loss when slowing down in a heavy water moderator. Therefore, after a limited number of collisions, they would easily escape from the molybdenum capture cross section resonance region, whenever not absorbed.

Similarly to the previous case considered, a preliminary parametric study has been performed to assess the required size for the lead buffer under the aforementioned proton beam operating conditions. From the former experience gained in the modeling of the proposed TRASCO RFQ-driven activator system, the best position where to arrange the samples to be irradiated is close to the cylindrical surface that holds both the W neutron converter and the related coaxial light water cooling pipes (see Figure 20). In such a position one (or more) molybdenum samples may be located, here considered as cylindrical thin shells.

In an empty volumetric region (cylindrical shell) surrounding the target holder having inner radius r = 5.5 cm, height h = 11 cm and thickness t= 0.1 cm, the volume-averaged neutron fluence per unit neutron source has been calculated in the three main energy ranges: the thermal group (E_n < 1 eV), the epithermal group (1 eV <E_n <100 keV), where Mo cross section resonances are entirely included and, finally, the fast group (E_n> 100 keV). In Figure 22, the normalized neutron fluence, as well as the spectral ratio for the epithermal neutrons only is plotted against the half-length of Pb cubic buffer which, roughly, is representative of the moderator thickness in the radial direction.

The results point out that the spectral ratio approaches the asymptotic value of about 0.26, when the cubic lead buffer reaches about 1.5 m size. Such a result is similar to what reported in the paper by

Froment et al. [14] for the neutron activator system developed, although the mass required turns out to be about 38 tons. However, since the epithermal spectral ratio improvement is about 8% only (corresponding to ~ 10% fluence drop) in the last 45 cm outer thickness, the final configuration for the cubic Pb buffer can be limited to 60 cm size, thus greatly reducing the required mass to about 2.5 tons.

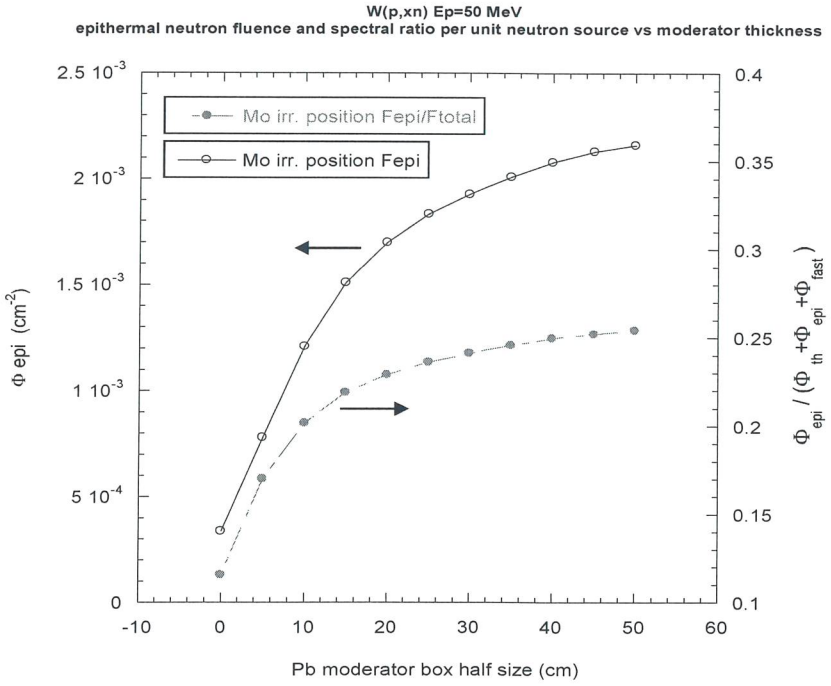

Fig. 22 Normalized neutron fluence (void circle black curve) and related spectral ratio (full circle red curve) in the epithermal energy range (1 eV <En< 100 keV) available in the sample irradiation site, with the proposed SPES-cyclotron driven neutron activator system. The x-axis parameter is the half of Pb buffer cubic size around the target. The statistical calculation errors are less than 0.1%.

Once set a trade-off for the optimal Pb buffer size, a RG-graphite reflector was then considered. The optimal thickness was estimated, likewise the TRASCO-RFQ driven system previously modeled, by calculating the volume-averaged ^{99}Mo production rate, expected at saturation, in a ^{98}Mo-enriched cylindrical sample placed at the irradiation site. The results are plotted in Figure 23, normalized both per unit volume and source neutron, versus RG-graphite moderator thickness surrounding the Pb buffer. An improvement in the ^{98}Mo(n,γ) production rated 15% only may be achieved, with an almost asymptotic condition, when the reflector thickness at least of 40 cm is taken into account. The gain in the last 20 cm thickness being about 1% only, the minimum RG-graphite size required is at last 20 cm. The activator overall dimensions estimated are therefore (L, W, H) (105x105x100) cm^3.

The normalized neutron fluence spectra, calculated at the sample irradiation position, are shown in Figure 24, considering both the bare target only (without Pb buffer and RG-graphite reflector) and the complete system. The resulting spectral configuration for such a system is optimized, having a nearly flat trend in the 1 eV-100 keV energy range, which integral is $2.19 \cdot 10^{-3}$ cm^{-2}. Reminding that the neutron source yield expected by the SPES-cyclotron-driven W neutron converter under operating conditions (see § 1.2.2) is $2.3 \cdot 10^{14}$ s^{-1}, an epithermal neutron flux level $\Phi_{epi} \sim 5.0 \cdot 10^{11}$ cm^{-2}s^{-1} would be reached in the sample irradiation position.

Finally, to test the effectiveness of the proposed activator system based on the SPES cyclotron, a performance comparison with the aforementioned activator system (see page 11) at JRC Ispra lab [15] was performed as well. The spectral characteristics are shown in Figure 25.

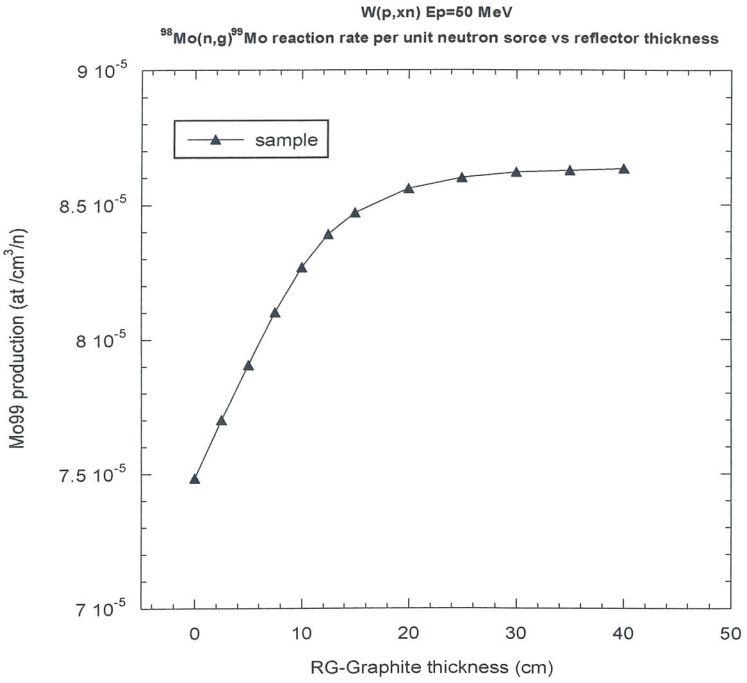

Fig. 23 Normalized ^{99}Mo production expected by (n,γ) reactions on ^{98}Mo (100% enrichment) samples with the proposed SPES-cyclotron driven neutron activator system versus the RG-graphite reflector thickness. The statistical calculation errors, not visible in the plot, are less than 0.1%.

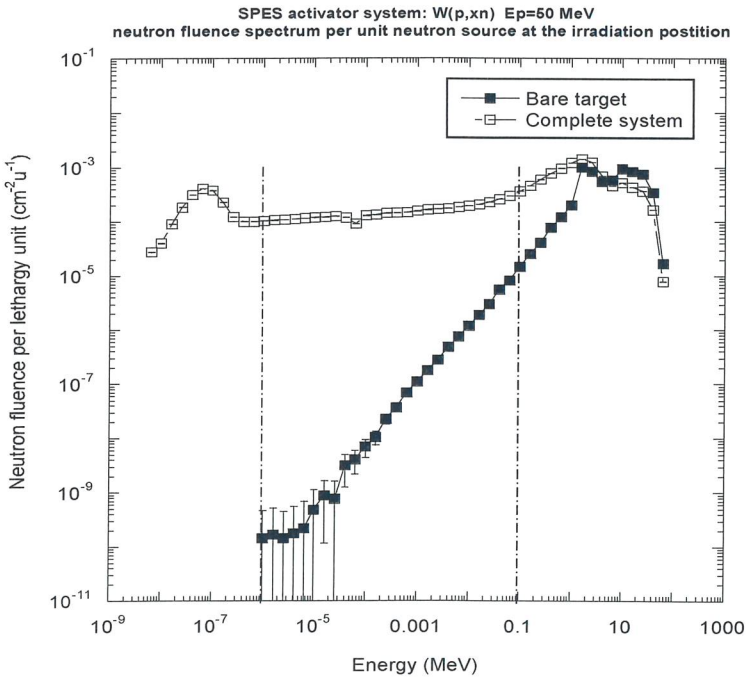

Fig. 24 Normalized neutron fluence spectra comparison which would be available at the sample irradiation position. The spectrum due to the bare W target only (full square plot), as well as the one considering the complete irradiation configuration (void square plot) are shown.

As expected, the analysis of the normalized spectra for both activator configurations shows a similar trend. Such a behavior points out that the proposed system, is able to provide, at the sample irradiation position, the same spectral quality in the epithermal energy range (even better at lower energies) when compared to the JRC activator system. By integrating the normalized neutron fluence plots in the 1 eV–100 keV energy intervals, the configuration proposed turns out to be about a factor of 3 better than the JRC one.

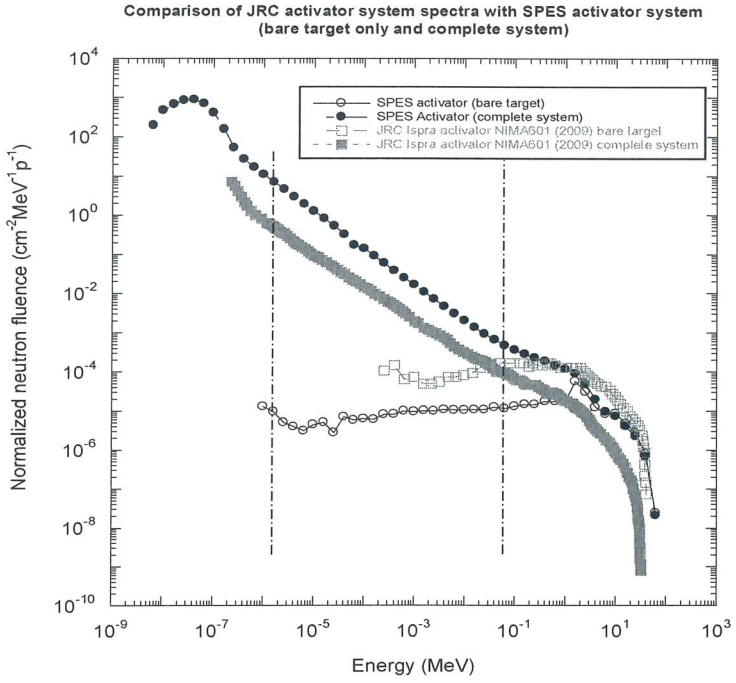

Fig. 25 Neutron fluence spectra comparison at the sample irradiation positions, normalized per unit energy and unit proton hitting the target, between the JRC activator system (red sqare plots) [15] and the proposed system based on the SPES cyclotron (black circle plots). Neutron spectra which would be available concerning the bare target only, as well as and the complete systems, are shown.

Such a better performance partially depends (about 2/3 out of the total contribution) on the improved n/p conversion efficiency, corresponding to $4.51 \cdot 10^{11}$ n/s·μA (see data on page 10 and ref. [13]), which can be obtained from W target hit by 50 MeV proton beam. The neutron yield from Be target under 40 MeV proton beam is $2.09 \cdot 10^{11}$ n/s·μA (see Table 1 and ref. [15]). The remaining part (approximately 1/3 out of the total) is instead from the improved system efficiency.

2.3.2. Expected ^{99}Mo production with SPES cyclotron-driven neutron activator

On the basis of such a preliminary modeling the ^{99}Mo production expected, at the End of Bombardment (EOB) inside ^{98}Mo-enriched irradiated sample may be, at last, estimated with a good accuracy level. The following table shows the main reference parameters and the estimated in-target specific activity calculated either after the first 24 hours of irradiation, or after a longer irradiation time corresponding to saturation.

As may be noted, by comparing the performance of the system concerned, with the former one investigated based on the RFQ TRASCO driver, an increasing reaction rate of a factor 5 only (i.e. an improved production capacity in the irradiated sample) might be reached. By increasing the proton beam energy from 50 up to the maximum 70 MeV allowed by SPES cyclotron (see page 10) the neutron yield improvement should approximately double. The expected ^{99}Mo production should therefore be

roughly an order of tenth larger. Moreover, because of a wider neutron energy spectrum, the additional ^{99}Mo production route exploiting the (n,2n) reaction channel (see section 1.2.3) has also been estimated from ^{100}Mo-enriched sample, the results of which are also enlisted in the table. However, as known (see § 1.2.1), the drawback is the ^{99}Mo production with some radionuclide contaminants.

Activator System based on SPES cyclotron (Ep=50 MeV) + W target			
SPES cyclotron output energy	Ep	50	MeV
proton beam current max.	Ip	0.5	mA
Beam power on target	P	25	kW
Neutron converter material		W	
Estimated total neutron output	$S_{n\,tot}$	$2.3 \cdot 10^{14}$	s^{-1}
Epithermal neutron fluence rate (1eV-100 keV) at sample position	Φ_{epi}	$5.0 \cdot 10^{11}$	$cm^{-2}\ s^{-1}$
TOTAL neutron fluence rate at sample position	Φ_{tot}	$1.9 \cdot 10^{12}$	$cm^{-2}\ s^{-1}$
Irradiated sample: ^{98}Mo/^{100}Mo (enrichment)	%	100	
Production route	**Mo98(n,γ)Mo99**		
Estimated TOTAL Reaction Rate (RR) inside sample		$1.93 \cdot 10^{10}$	$cm^{-3}\ s^{-1}$
RR fraction due to epithermal neutrons (1eV-100 keV)	%	81.3	
^{99}Mo Specific Activity at saturation ($T_{irr} \cong 5\ \tau \cong 20$ d)	As*	50.8	mCi/g
^{99}Mo Specific activity (first 24 hrs)	As	11.3	mCi/g
^{98}Mo bulk mass requested for 1 Ci ^{99}Mo production (first 24 hrs)	m	~90	g
Production route	**Mo100(n,2n)Mo99**		
Estimated TOTAL Reaction Rate (RR) inside sample		$1.31 \cdot 10^{10}$	$cm^{-3}\ s^{-1}$
RR fraction due to fast neutrons (En > 100 keV)	%	100.0	
^{99}Mo Specific Activity at saturation ($T_{irr} \cong 5\ \tau \cong 20$ d)	As*	34.5	mCi/g
^{99}Mo Specific activity (first 24 hrs)	As	7.7	mCi/g
^{98}Mo bulk mass requested for 1 Ci ^{99}Mo production (first 24 hrs)	m	~130	g

Additional open reaction channels: **many, even with long mean lifetime, i.e.: Sr90 (β-) $T_{1/2}$ =28y → Y90**

From the parameters calculated through MCNPX simulation, the *effective* microscopic cross-section value, σ_{eff}, may now be weighted for the energy range of resonances. Such a value must be used in simplified calculations to estimate correctly the ^{99}Mo production in the epithermal energy range. Similarly to the former study performed for the TRASCO RFQ based activator system, the ^{98}Mo(n,γ) reaction rate calculated is as follows:

$$Y^{99Mo} = \int_{1eV}^{100\,keV} n_{98_{Mo}}\,\sigma(E)\Phi(E)dE = 1.93 \cdot 10^{10} \cdot 0.813 = 1.57 \cdot 10^{10}\mathrm{cm}^{-3}\mathrm{s}^{-1}$$

$$\sigma_{epi\,eff} = 0.049 \cdot 10^{-23}\ cm^2 \approx 0.5\ barn$$

The flux-weighted cross section mean value, $\sigma_{epi\,eff}$, taking into account the entire energy range, is instead just ~ 0.16 barn. Weighted cross section value as low as indicated means that very thin samples to be irradiated are not required. Even with relatively large thickness (1-5 mm), local neutron flux drops inside the material are not produced, thus guaranteeing a homogeneous activation within the sample.

2.4. SPES cyclotron proton-driven ^{99}Mo and ^{99m}Tc direct production

As enlisted in Part I, the ^{99}Mo production at LNL might also be obtained through the ^{100}Mo(p,pn)^{99}Mo reaction using the SPES cyclotron as proton driver. In such a feasibility study the irradiation configurations in which the minimum (40 MeV) as well as the maximum (70 MeV) protons energy is used, have been taken into account. The production level expected at the End of Bombardment (EOB) on ^{100}Mo-enriched (100%) thick-targets (samples) have been estimated and reported as reference parameters.

The other interesting reaction channel ^{100}Mo(p,2n)^{99m}Tc is also known (see § 1.3.1) to be allowed at proton energies exceeding 10 MeV. However the direct ^{99m}Tc production with good quality level is expected only when the starting energy is in the range Ep = 22-25 MeV. In such a way, while slowing down inside target thickness, protons would fully cross the energy range where the reaction rate probability is large, being the ^{100}Mo(p,2n) cross-section peak around 250-300 mb at 15 MeV. Although the minimum output energy (40 MeV) provided by the SPES cyclotron is even higher than required, an estimate of ^{99m}Tc yield expected in such an irradiation condition is however given, as well as at the optimal 25 MeV, considering the insertion of an energy degrader.

2.4.1. Main proton beam parameters and ^{99}Mo/^{99m}Tc yield distribution inside sample

The nuclides production may be basically outlined as in the following sketch shown in Figure 26.

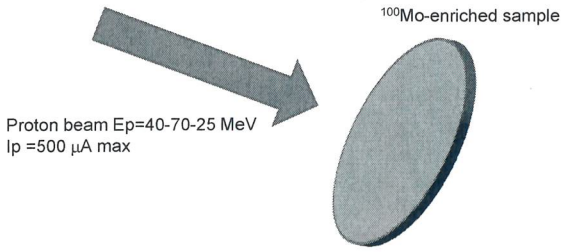

Fig. 26 Proof-of-principle scheme for ^{99}Mo/^{99m}Tc direct production using ^{100}Mo sample target.

The proton beam hits the molybdenum sample in normal direction and is fully stopped within the thickness (thick-target configuration). In such irradiation conditions the required thickness for the molybdenum material has to be primarily assessed both at the minimum and the maximum protons energy, in order to limit the amount and, consequently, the material cost. Detailed tabulated data on stopping power values, as well as projected ranges, for protons in molybdenum may be easily taken from the PSTAR database of the National Institute for Standards and Technology (NIST) website [37]. Such

data have been calculated using the methods described in ICRU-37 [38] and ICRU-49 [39] reports. The values, normalized to natural molybdenum bulk density, (ρ = 10.28 gcm^{-3}), are shown in Figure 27.

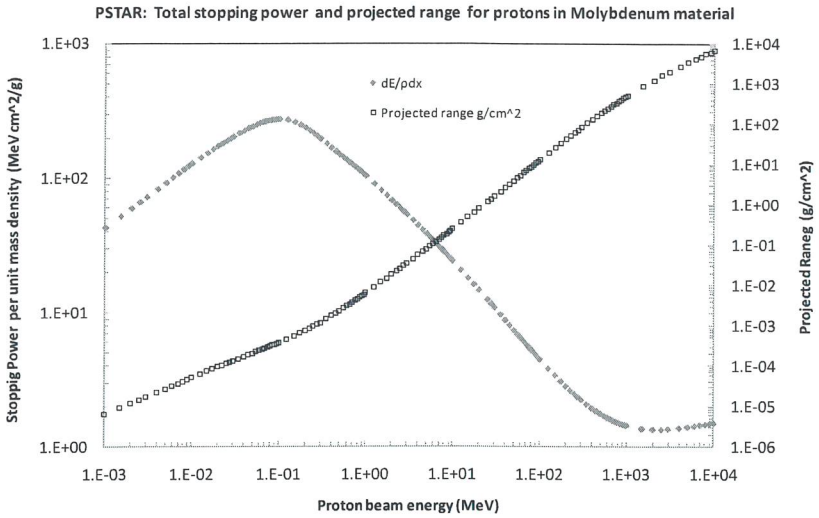

Fig. 27 Stopping power and projected range for natural molybdenum against the proton energy. Source database: PSTAR (NIST) [37].

As it can be estimated, 70 MeV protons are fully stopped within 7.1 mm thickness, while 2.7 mm are instead needed with 40 MeV protons. On the other hand, when the hitting energy is even lower, 25 MeV, optimized for ^{99m}Tc production, 1.25 mm are enough to fully stop the beam. The energy losses per unit path of protons crossing Mo, as well as the corresponding protons energy drop off versus the penetration depth inside the target thickness, are shown in the Figure 28 for both the lower and upper cyclotron output energy. In the next Figure 29 the same data are plotted for 25 MeV protons. The behavior in all the cases considered is similar: a nearly flat energy loss in the first millimeters depth, followed by a sharp increase corresponding to the Bragg peak.

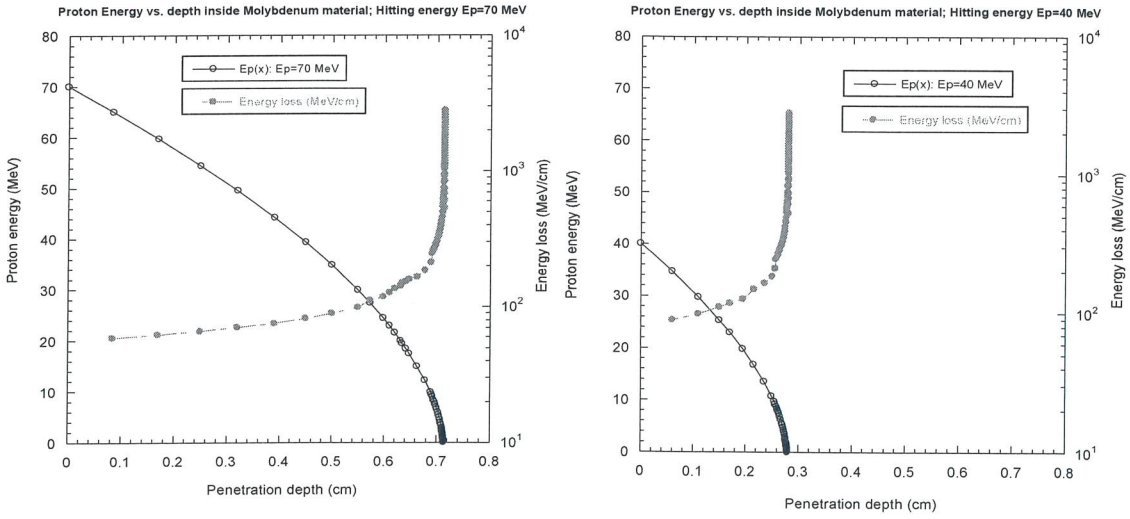

Fig. 28 Energy loss per unit length (red full circle) and corresponding energy reduction (black open circle) versus protons penetration depth inside molybdenum. Two irradiation configurations are considered: Ep = 70 MeV (left plot) and Ep = 40 MeV (right plot). Note the very narrow Bragg peak in both cases.

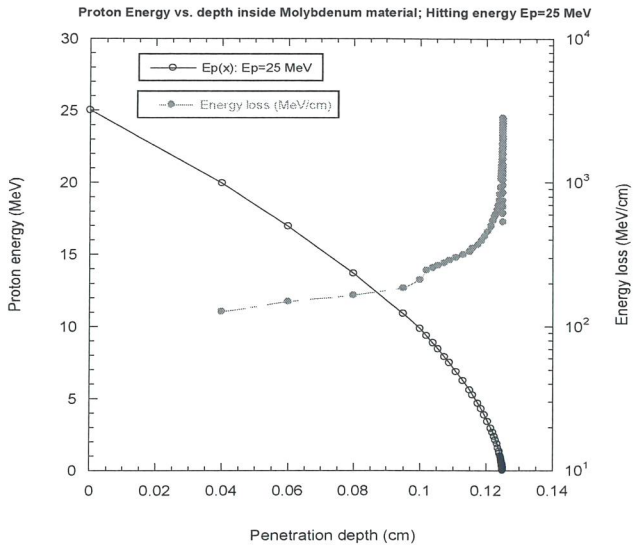

Fig. 29 Energy loss per unit length (red full circle) and corresponding energy reduction (black open circle) versus penetration depth inside molybdenum for 25 MeV protons.

The ^{99}Mo yield distribution within the sample thickness may be calculated by the experimental ^{100}Mo(p,xn) excitation function data measured by Schölten et al. [3, 40], retrieved by the Experimental Nuclear Reaction Data at EXFOR (CSISRS) database. Among the most recent and reliable measurements, they are the only ones that cover the whole energy range of interest up to 70 MeV, whose values are shown in the Figure 30.

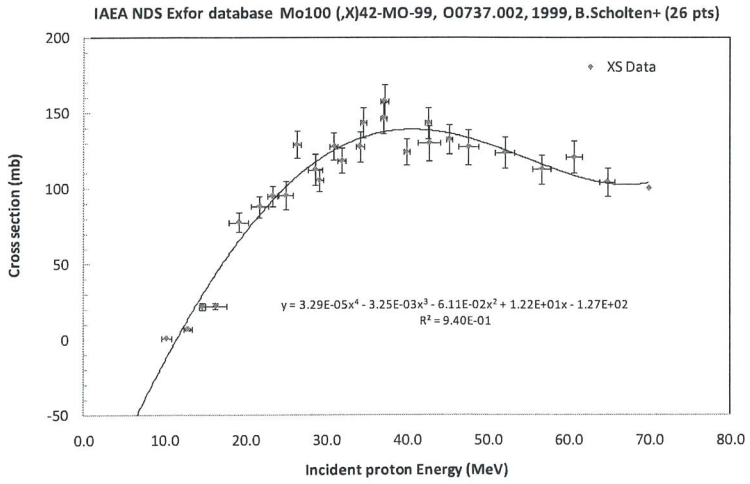

Fig.30 Experimental excitation functions data for ^{100}Mo(p,x)^{99}Mo reaction: EXFOR format, IAEA-Nuclear Data System [40].

Since the target thickness T_0 required to fully stop the beam is much lower than the maximum linear dimension (radius) of the cylindrical sample, (as usually occurs supposing a beam power areal density of the order of some hundreds W/cm^2), a calculation approach based on a slab geometry model (see sketch below) may be used in this case with good approximation, as schematically shown in Figure 31.

Given an infinitesimal thickness dt, placed at depth t from the sample hitting surface, where a constant energy value may be assumed for protons, the local contribution to the overall reaction rates is described by the equation below:

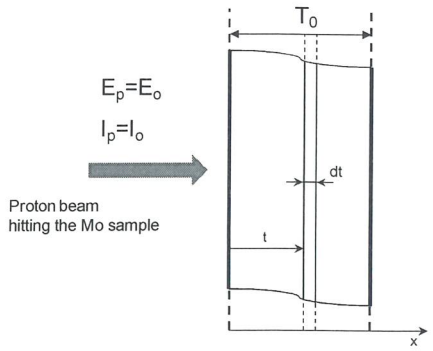

Fig. 31 Main geometric parameters in slab approximation geometry for the calculation of reaction rates distribution inside the target thickness.

$$dY^{99Mo} = \Sigma_{100_{Mo}}(\mathrm{E(t)}) \cdot \Phi(E(t))dV = n_{100_{Mo}}\sigma\left(E_0 - \int_0^t \frac{dE}{dx}\,dx\right)\left(\frac{I_o}{Q}e^{-n_{100_{Mo}}\sigma_R\left(E_0 - \int_0^t \frac{dE}{dx}dx\right)dt'}\right)_t dt$$

where: I_o = proton beam current hitting the sample;
Q = electric charge unit;
σ = ^{100}Mo(p,pn)^{99}Mo microscopic cross section;
σ_R = microscopic removal cross section (all reaction channels that remove protons from main stream: basically we assume the three main reaction channels for ^{99}Mo e ^{99m}Tc and ^{99g}Tc production.

The expression within brackets represents the protons flux level available at the generic depth t inside sample, whose exponential contribution takes into account the attenuation of the beam at different depths. However, considering the cross section order of tenth involved (see Figure 29), the contribution of the exponential, for each infinitesimal thickness inside sample, is practically constant, equal to unity. Therefore, the former expression may be simplified in the following one without making significant errors:

$$dY^{99Mo} = \Sigma_{100_{Mo}}(\mathrm{E(t)}) \cdot \Phi(E(t))dV = n_{100_{Mo}}\sigma\left(E_0 - \int_0^t \frac{dE}{dx}\,dx\right)\cdot\frac{I_o}{Q}dt$$

By integrating over the whole target thickness, once divided by the number of protons per unit time hitting the target, $n_p = Io/Q$, the overall nuclide production, normalized for incident proton, may be obtained:

$$\frac{Y^{99Mo}}{n_p} = n_{100_{Mo}}\int_0^{T_0}\sigma\left(E_0 - \int_0^t \frac{dE}{dx}\,dx\right)\cdot dt$$

The radionuclides yield trends expected inside sample thickness at 40, 70 MeV and 25 MeV, normalized per hitting proton, are at last plotted in Figure 32.

As can be noted the radionuclide production remains barely constant inside sample thickness, down to the point in which the energy loss starts increasing towards the Bragg peak. The recommended thickness in order to get an optimized ^{99}Mo production without the useless heat power deposition in such a

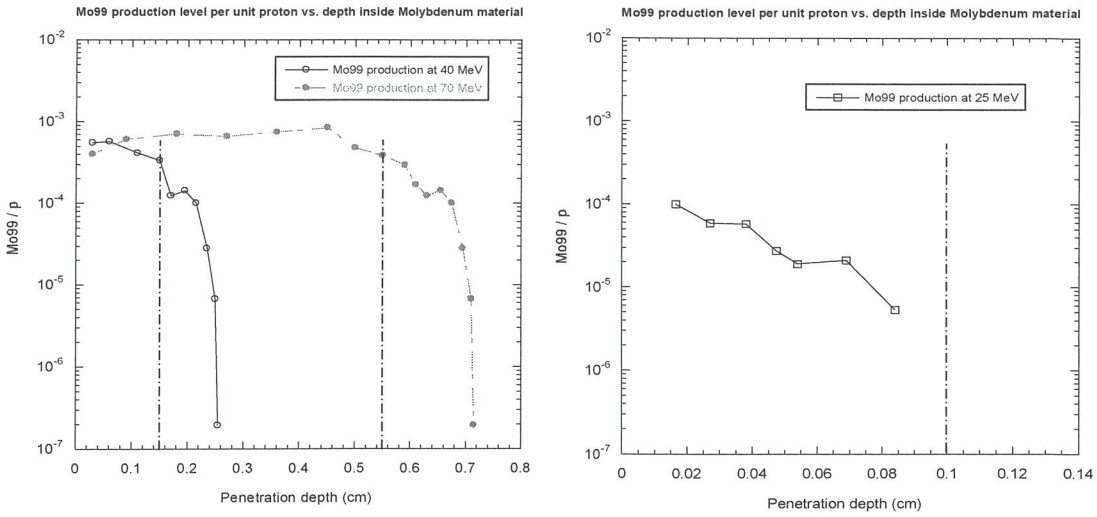

Fig. 32 Distribution of ^{99}Mo yield per hitting proton, versus penetration depth, inside ^{100}Mo-enriched samples for proton beam energies of 40 and 70 MeV (left plot) and 25 MeV (right plot). The vertical dash-dotted lines are the recommended sample thicknesses to get an optimized ^{99}Mo production avoiding the Bragg peak inside the sample. The ^{99}Mo production at 25 MeV is however of little or no significance.

region are, therefore, 1.5 mm at 40 MeV and 5.5 mm at 70 MeV. When 25 MeV protons are instead used, the production drops off before the optimal thickness of 1.0 mm is reached. The overall ^{99}Mo production in such a case is of no or little significance.

The integral for ^{99}Mo production, normalized per hitting proton, estimated at EOB inside samples at the three proton energy levels considered, are at last enlisted in the table below both at thin and thick target configurations:

protons energy	99Mo/p thick target production (full beam stopped)	99Mo/p thin target production (Bragg peak out)
Ep =70 MeV	$4.95 \cdot 10^{-3}$	$4.34 \cdot 10^{-3}$
Ep =40 MeV	$1.50 \cdot 10^{-3}$	$1.09 \cdot 10^{-3}$
Ep =25 MeV	$3.035 \cdot 10^{-4}$	$3.035 \cdot 10^{-4}$

When the direct ^{99m}Tc production is instead taken into consideration, either at the minimum 40 MeV energy allowed by SPES cyclotron, or at the optimized 25 MeV after beam energy degradation, the combined experimental excitation function measurements by Scholten et al. [3.41] and Tackas et al. [4.42], are taken into account and shown in Figure 33. On the other hand, to make an estimation of the ground state ^{99g}Tc production expected the only one excitation function so far available from TENDL2009 library (uniquely derived from theoretical models) has been considered, which is shown in the next Figure 34. Also plotted is the cross sections ratio, $\sigma^{99gTc}/\sigma^{99mTc}$, which shows some fluctuations mainly depending on the oscillations in the experimental points at energies higher than 30 MeV. For proton energies between 25 MeV down to 10 MeV, the reaction rate ratio for the production of both nuclides is thus expected to be within 3 and 4.

Provided that such a theoretical excitation function is reliable, there is only a small energy window as may be noted, ranging from 25 MeV down to about 18-19 MeV, which could meet the requirement for an accelerator-driven ^{99m}Tc production quality, being the minimum production rate ratio about 3.2 at 21.5 MeV. Despite the favorable irradiation parameters, the N^{99gTc}/N^{99mTc} atomic ratio that would result inside samples at EOB is however close to the aforementioned limiting factor (see § 1.3.1), even after quite a short irradiation time (i.e. $T_{irr} < \frac{1}{2}\ T_{1/2}$). This is because of the additional ^{99g}Tc contribution,

either from ^{99m}Tc decay, or directly from decay of the ^{99}Mo generated. This aspect might at last be an issue, which may be assessed with imaging *in-vivo* tests to find-out the still acceptable limit.

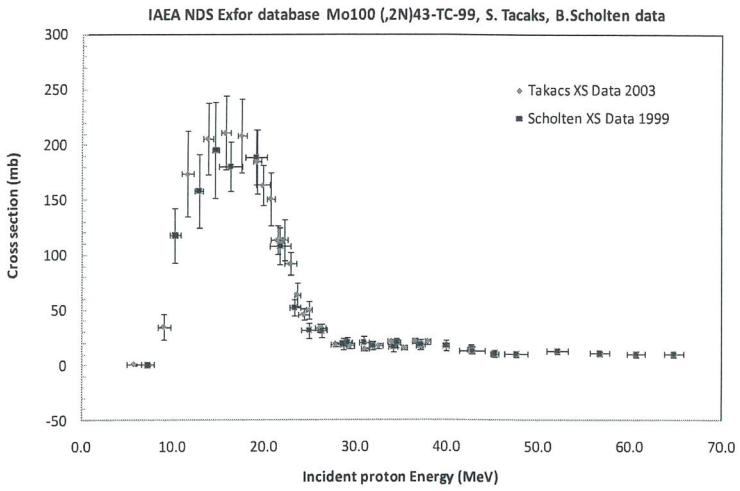

Fig. 33 Experimental excitation functions data for ^{100}Mo(p,2n)^{99m}Tc reaction: EXFOR format, IAEA-Nuclear Data System [39,40].

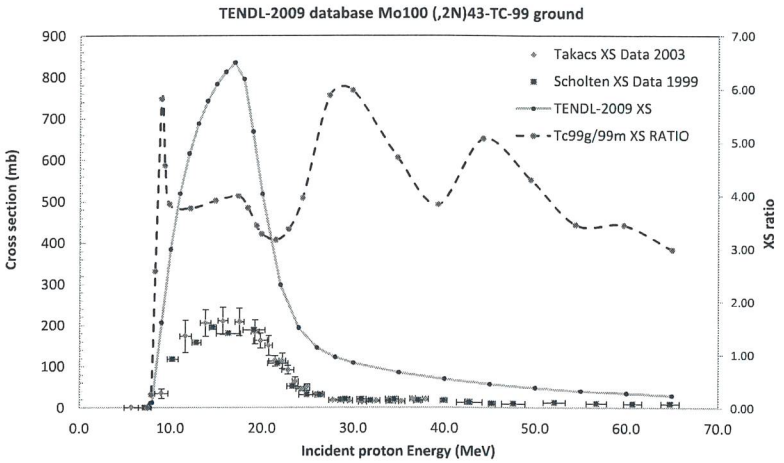

Fig. 34 Theoretical excitation function for the pure β-emitter ground state ^{99g}Tc production by the same ^{100}Mo(p,2n) reaction from TENDL2009 library [30], compared to the experimental ones for ^{99m}Tc of Figure 33. The cross section ratio for both reactions expected at different proton energies is also plotted.

In order to get a reference, when technetium ($^{99m+g}$Tc), under pertechnetate form (TcO_4^-), is spilled out (washed) as sterile solution from a standard Mo/Tc generator after each 24 hrs interval, the maximum ^{99m}Tc activity is reached, as shown in the next Figure 35 (top). The corresponding N^{99gTc}/N^{99mTc} atomic ratio estimated in transient equilibrium at that time between the two isomers turns out to be about 2.5. When the accelerator-produced technetium is instead considered within the best proton energy range (25 - 19.5) MeV, preliminary integral yields calculations have shown that a ^{99g}Tc/^{99m}Tc ratio about 3.3 is expected. Taking into account the aforementioned additional ^{99g}Tc contribution as decay product, the resulting net N^{99gTc}/N^{99mTc} atomic ratio at EOB would be estimated around 4.0 just after 3 hours irradiation (see Figure 35, bottom). Such considerations might therefore suggest a series of shorter time irradiations (1.5-2 hrs maximum) on a few (2-3) samples, than only one for a longer period (3-6 hrs) on a single sample.

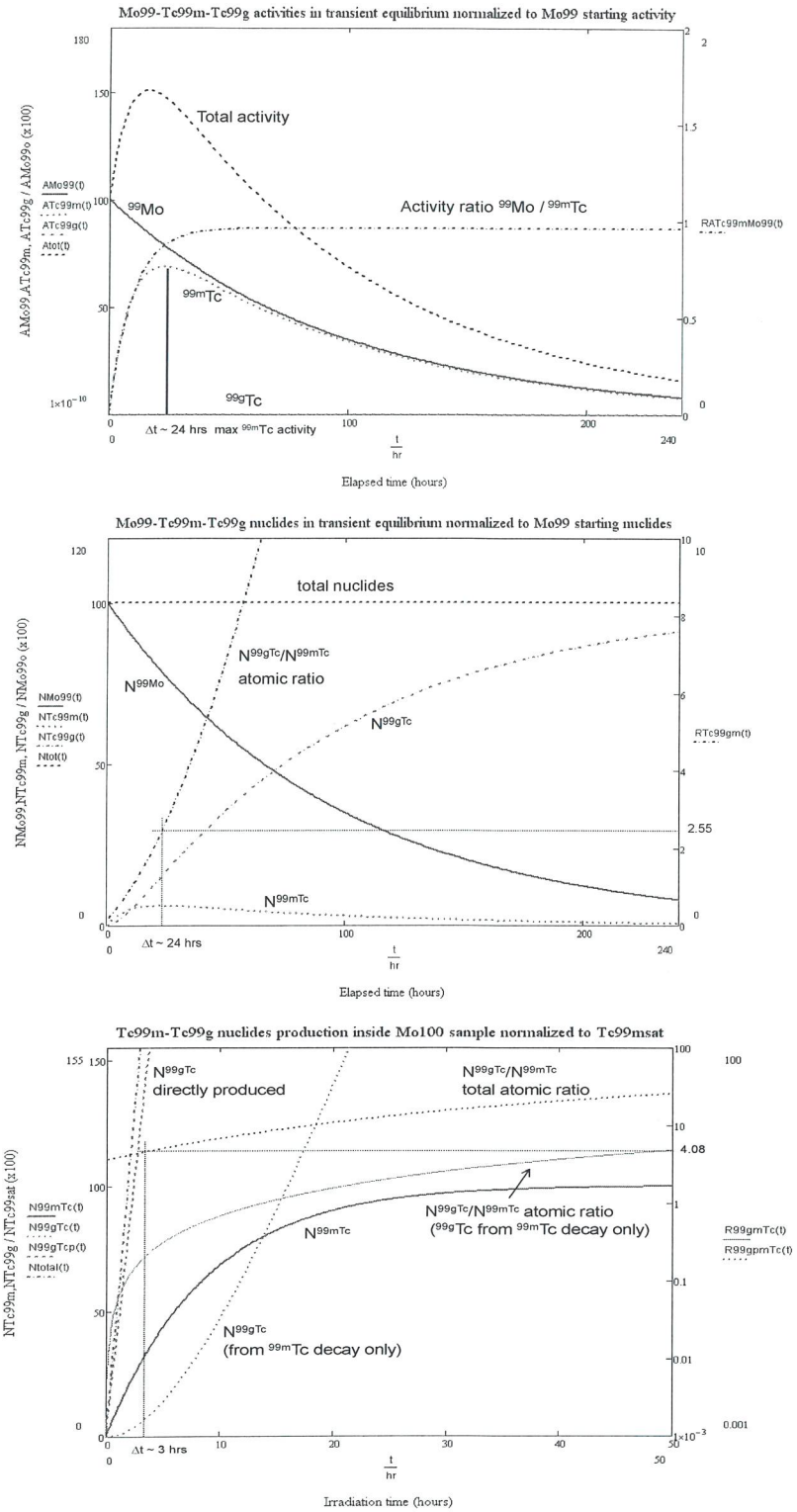

Fig. 35 (Top) ^{99m}Tc, ^{99g}Tc, ^{99}Mo decay activities, as well as their total (normalized to ^{99}Mo starting decay activity) versus time usually available in transient equilibrium inside Mo/Tc generators in case no technetium is spilled out from. Also plotted is the activity ratio between ^{99}Mo and ^{99m}Tc. (Middle) Corresponding atom fractions available for same nuclides (normalized to ^{99}Mo stating nuclides). The ratio between technetium isomeric states ^{99g}Tc/^{99m}Tc is also shown. (Bottom) ^{99m}Tc, ^{99g}Tc build up nuclides (normalized to ^{99m}Tc at saturation) expected inside a ^{100}Mo fully enriched sample at EOB versus irradiation time. ^{99g}Tc/^{99m}Tc integral yields ranging 3.29 estimated within the proton energy range (25-19.5) MeV is taken into account. The additional (negligible) contribution of ^{99g}Tc and ^{99m}Tc as decay products of ^{99}Mo produced is here not considered.

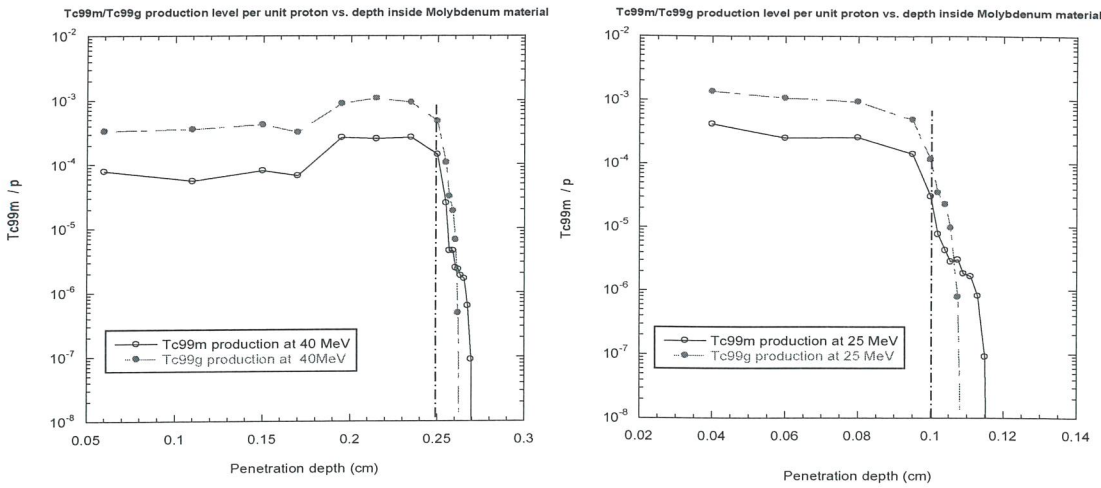

Fig. 33 Distribution of ^{99m}Tc and ^{99g}Tc normalized productions, versus penetration depth, inside ^{100}Mo-enriched samples for proton beam energies at 40 MeV (left plot) and 25 MeV (right plot). The vertical dash-dotted lines are the recommended sample thicknesses to get an optimized $^{99m+g}$Tc production avoiding the Bragg peak inside the sample. At 25 MeV the ^{99}Mo production is instead of little or no significance.

The ^{99m}Tc/^{99g}Tc yield distribution estimated inside sample thickness is at last plotted in the next Figure 36, when 40 MeV as well as 25 MeV proton beams are taken into account. In such a case the integral yields for ^{99m,g}Tc, normalized per hitting proton, estimated at EOB inside samples at two proton energy levels considered, are enlisted in the following table both at thin and thick target configurations. The N^{99gTc}/N^{99mTc} yield ratios expected are also reported. The additional contribution of ^{99g}Tc and ^{99m}Tc as decay products of negligible amount of ^{99}Mo produced is here not considered.

protons energy		99mTc/p production	99gTc/p production	99gTc /99mTc yield ratio
Ep =40 MeV	thick target	$1.227 \cdot 10^{-3}$	$4.984 \cdot 10^{-3}$	4.061
Ep =40 MeV	thin target	$1.171 \cdot 10^{-3}$	$4.787 \cdot 10^{-3}$	4.087
Ep =25 MeV	thick target	$9.208 \cdot 10^{-4}$	$3.366 \cdot 10^{-3}$	3.655
Ep =25 MeV	thin target	$8.959 \cdot 10^{-4}$	$3.287 \cdot 10^{-3}$	3.669

2.4.2. ^{99}Mo/^{99m}Tc direct production expected

Similarly to the previous cases analyzed, the production expected by ^{100}Mo thick-target direct irradiation with protons at different energies may be estimated separately, taking Into account the two reaction routes; the ^{99}Mo at both 40 and 70 MeV protons, while the ^{99m}Tc at 40 and 25 MeV. Since the beam power level hitting the molybdenum sample is not negligible, causing the sample melting whether a proper cooling is not provided, in this preliminary study a mean power areal density of 500 W/cm^2 has been considered as reference. The proton beam spot size and energy thus resulting uniquely defines the size and mass of thick samples requested, as well as the specific and/or concentration activities expected.

In the following tables, the main parameters estimated, both for the first 24 hrs irradiation, and at saturation level, are enlisted for thick samples configuration.

Case 1: ^{99}Mo production with Ep= 70 MeV, Ip= 500 μA
Preliminary design assumption for mean power areal density on sample: 500 W/cm^2

Direct 99Mo production using SPES cyclotron (Ep = 70 MeV)			
SPES cyclotron output energy	Ep	70	MeV
Proton beam current	Ip	0.5	mA
Beam power on sample (target)	P	35	kW
^{100}Mo sample: enrichment	%	100	
Production system		Mo100(p,pn)Mo99	
Estimated TOTAL Reaction Rate (RR) inside sample		$1.54 \cdot 10^{13}$	s^{-1}
^{99}Mo integral yield at saturation inside sample per unit proton current ($T_{irr} \cong 5\,\tau \cong 20$ days)	$\overline{A_S}$	834.8	mCi/μA
^{99}Mo integral yield inside sample per unit proton current ($T_{irr} < \tau/4 = \sim 24$ hrs)	$\overline{A'}$	7.75	mCi/μAh
Mo sample disc (target) size at the fixed beam power density		R=4.72 cm, s= 0.71 cm V=49.96 cm^3, M =513.6 g	
Available ^{99}Mo activity inside sample (first 24hrs)	A	93.1	Ci
^{99}Mo Specific activity (first 24hrs)	As	181.2	mCi/g
^{99}Mo Specific activity at saturation ($T_{irr} \cong 5\,\tau \cong 20$ days)	As*	812.7	mCi/g
Additional open reaction channels: **many, even with long mean lifetime, i.e.: Sr90 (β-) $T_{1/2}$ =28y -→ Y90**			

Case 2: ^{99}Mo production with Ep= 40 MeV, Ip= 500 μA
Preliminary design assumption for mean power areal density on sample: 500 W/cm^2

Direct 99Mo production using SPES cyclotron (Ep = 40 MeV)			
SPES cyclotron output energy	Ep	40	MeV
Proton beam current	Ip	0.5	mA
Beam power on sample (target)	P	20	kW
^{100}Mo sample: enrichment	%	100	
Production system		Mo100(p,pn)Mo99	
Estimated TOTAL Reaction Rate (RR) inside sample		$4.67 \cdot 10^{12}$	s^{-1}
^{99}Mo integral yield at saturation inside sample per unit proton current ($T_{irr} \cong 5\,\tau \cong 20$ days)	$\overline{A_S}$	252.3	mCi/μA
^{99}Mo integral yield inside sample per unit proton current ($T_{irr} < \tau/4 = \sim 24$ hrs)	$\overline{A'}$	2.34	mCi/μAh
Mo sample disc (target) size at the fixed beam power density		R=3.57 cm, s= 0.27 cm V=10.98 cm^3, M =112.8 g	
Available ^{99}Mo activity inside sample (first 24hrs)	A	28.1	Ci
^{99}Mo Specific activity (first 24hrs)	As	249.2	mCi/g
^{99}Mo Specific activity at saturation ($T_{irr} \cong 5\,\tau \cong 20$ days)	As*	1117.9	mCi/g
Additional open reaction channels: **many, even with long mean lifetime, i.e.: Sr90 (β-) $T_{1/2}$ =28y -→ Y90**			

Case 3: ^{99m}Tc production with Ep= 40 MeV, Ip= 500 μA
Preliminary design assumption for mean power areal density on sample: 500 W/cm^2

Direct ^{99m}Tc production using SPES cyclotron (Ep = 40 MeV)			
SPES cyclotron output energy	Ep	40	MeV
Proton beam current	Ip	0.5	mA
Beam power on sample (target)	P	20	kW
^{100}Mo sample: enrichment	%	100	
Production system		Mo100(p,2n)Tc99m	
Estimated TOTAL Reaction Rate (RR) inside sample		$3.83 \cdot 10^{12}$	s^{-1}
^{99m}Tc integral yield at saturation inside sample per unit proton current ($T_{irr} \cong 5\,\tau \cong 45$ hrs)	$\overline{A_S}$	207.1	mCi/μA
^{99m}Tc integral yield inside sample per unit proton current ($T_{irr} < \tau/2 = \sim 4$ hrs)	$\overline{A'}$	19.1	mCi/μAh
Mo sample size disc (target) at the fixed power density		R=3.57 cm, s= 0.27 cm V=10.98 cm^3, M =112.8 g	
Available ^{99m}Tc activity inside sample (first 24hrs)	A	97.0	Ci
^{99m}Tc activity concentration (first 24hrs)	As	859.9	mCi/g
^{99m}Tc activity concentration at saturation ($T_{irr} \cong 5\,\tau \cong 45$ hrs)	As*	917.5	mCi/g
Additional open reaction channels: **many, even with long mean lifetime, i.e.: Sr90 (β-) $T_{1/2}$ =28y → Y90**			

Case 4: ^{99m}Tc production with Ep= 25 MeV, Ip= 500 μA
Preliminary design assumption for mean power areal density on sample: 500 W/cm^2

Direct ^{99m}Tc production using SPES cyclotron (Ep = 25 MeV)			
SPES cyclotron output energy	Ep	25	MeV
Proton beam current	Ip	0.5	mA
Beam power on sample (target)	P	12.5	kW
^{100}Mo sample: enrichment	%	100	
Production system		Mo100(p,2n)Tc99m	
Estimated TOTAL Reaction Rate (RR) inside sample		$2.87 \cdot 10^{12}$	s^{-1}
^{99m}Tc integral yield at saturation inside sample per unit proton current ($T_{irr} \cong 5\,\tau \cong 45$ hrs)	$\overline{A_S}$	155.4	mCi/μA
^{99m}Tc integral yield inside sample per unit proton current ($T_{irr} < \tau/2 = \sim 4$ hrs)	$\overline{A'}$	14.4	mCi/μAh
Mo sample size disc (target) at the fixed power density		R=2.82 cm, s= 0.12 cm V=3.004 cm^3, M =30.9 g	
Available ^{99m}Tc activity inside sample (first 24hrs)	A	72.8	Ci
^{99m}Tc activity concentration (first 24hrs)	As	2357.0	mCi/g
^{99m}Tc activity concentration at saturation ($T_{irr} \cong 5\,\tau \cong 45$ hrs)	As*	2515.0	mCi/g
Additional open reaction channels: **many, even with long mean lifetime, i.e.: Sr90 (β-) $T_{1/2}$ =28y -→ Y90**			

2.5. Summary of calculation results and comparison with literature data

The following table summarizes a comparison of the main data between $^{99}Mo/^{99m}Tc$ yields measured in some experimental tests and reported in literature [3,4] with those estimated in the present study. The goal is to get indications about in-target production levels reasonably expected at EOB, after 24 hrs irradiation, with the different configurations analyzed under the constraints concerned.

Production route	$^{100}Mo(p,x)^{99}Mo$		$^{100}Mo(p,2n)^{99m}Tc$		$^{98}Mo(n,\gamma)^{99}Mo$		$^{100}Mo(n,2n)^{99}Mo$	
	ref [3,4]	SPES cyclotron	ref [3,4]	SPES cyclotron	ref [10,14,15]	TRASCO RFQ & SPES cyclotron neutron act.	ref [20,23]	SPES cyclotron neutron act.
	exp. meas.	prediction	Exp. meas.	prediction	Exp. meas.	prediction	Exp. meas.	prediction
$\overline{A_S}$ [mCi/μA] ($T_{irr} \cong 5\,\tau \cong 20$ d)	Ep = 40 MeV ? Ep = 65 MeV 750	Ep = 40 MeV 252 Ep = 70 MeV 835						
$\overline{A'}$ [mCi/μAh] ($T_{irr} < \tau/4 \cong 24$ hrs)	Ep = 40 MeV 3 - 4 Ep = 65 MeV 7.5	Ep = 40 MeV 2.3 Ep = 70 MeV 7.8						
$\overline{A_S}$ [mCi/μA] ($T_{irr} \cong 5\,\tau \cong 45$h)			Ep = 40 MeV ? Ep = 22 MeV 103	Ep = 40 MeV 207.1 Ep = 25 MeV 155				
$\overline{A'}$ [mCi/μAh] ($T_{irr} < \tau/2 \cong 4$ hrs)			Ep = 40 MeV 20.6 Ep = 22 MeV 11-17	Ep = 40 MeV 19.1 Ep = 25 MeV 14.4				
A_{S^*} [mCi/g] ($T_{irr} \cong 5\,\tau \cong 20$d)					20 - 40	TRASCO-RFQ 10.6 SPES cyclotron 50.8		
A_S [mCi/g] ($T_{irr} < \tau/4 \cong 24$ hrs)					?	TRASCO-RFQ 2.4 SPES cyclotron 11.3		
A_{S^*} [mCi/g] ($T_{irr} \cong 5\,\tau \cong 20$ d)							0.2 - 20	34.5
A_S [mCi/g] ($T_{irr} < \tau/4 \cong 24$ hrs)							?	7.7

At last in the first summary table below the $^{99}Mo/^{99m}Tc$ yields expected, as well as the ^{100}Mo enriched sample mass required are shown for all the production routes investigated. A more realistic 12 hrs/day beam time from accelerators is considered, shared with other experimental apparatuses at LNL, at the maximum beam current. In the following table the in-target yields expected at EOB, considering both thick and thin samples configuration, is instead reported for the same 12 hrs beam time, for $^{99}Mo/^{99m}Tc$ direct production, under the three proton energy levels considered.

Production route	Direct production (protons)		Induced production (neutrons)	
	$^{100}Mo(p,x)^{99}Mo$	$^{100}Mo(p,2n)^{99m}Tc$	$^{98}Mo(n,\gamma)^{99}Mo$	$^{100}Mo(n,2n)^{99}Mo$
	100% ^{100}Mo sample	100% ^{100}Mo sample	100% ^{98}Mo sample	100% ^{100}Mo sample
Accelerator	SPES Cyclotron Ip= 500 μA 500 W/cm^2 on sample	SPES Cyclotron Ip= 500 μA 500 W/cm^2 on sample	TRASCO RFQ Ip=30 mA Ep=5 MeV --- SPES Cyclotron Ip= 500 μA Ep=50 MeV	SPES Cyclotron Ip= 500 μA Ep=50 MeV
In-target Activity (EOB) [Ci] (12 hrs beam/day)	(Ep = 40 MeV) 15 --- (Ep = 70 MeV) 50	(Ep = 40 MeV) 78	TRASCO-driven activator 1.0 --- SPES cyclotron driven activator 1.0	SPES cyclotron driven activator 1.0
Sample mass required	(Ep = 40 MeV) 113 gr --- (Ep = 70 MeV) 514 gr	115 gr	795 gr --- 165 gr	245 gr

Production system	$^{100}Mo(p,x)^{99}Mo$		$^{100}Mo(p,2n)^{99m}Tc$	
	thick sample	thin sample	thick sample	thin sample
In-target Activity [Ci]	Ep = 70 MeV, 500 W/cm^2			
	49.5	43.4	--	--
Specific activity [mCi/g]	96.3	109.5	--	--
In-target Activity [Ci]	Ep = 40 MeV, 500 W/cm^2			
	14.9	10.9	77.6	74.0
Specific activity /Activity concentration [mCi/g]	132.5	174.8	720.2	687.5
In-target Activity [Ci]	Ep = 25 MeV, 500 W/cm^2			
	3.0	3.0	58.2	56.6
Specific activity /Activity concentration [mCi/g]	98.2	124.8	1884.6	2329.4

2.6. Conclusion

The following conclusions may at last be established, taking into account the constraints concerned:

a. The proposed activator system driven by the TRASCO RFQ accelerator would provide the ^{99}Mo with the best purity, having negligible contamination from other radionuclides. The neutron fluence level in the energy range (1 eV - 100 keV) where a very high fraction, about 90%, of ^{98}Mo(n,γ) neutron capture events occurs, is however poor. The resulting ^{99}Mo specific activities, both at saturation and after the first 24 hrs irradiation, are too much low to consider a massive production using such a system. High ^{98}Mo-enriched mass required for the irradiated sample:

- M= ~400gr to get 1 Ci in-target activity (EOB) due to ^{99}Mo production after 24 hrs irradiation;
- M= ~800gr to get 1 Ci in-target activity (EOB) due to ^{99}Mo production after 12 hrs irradiation.

b. The proposed activator system based on SPES cyclotron is able to provide better ^{99}Mo specific activities inside irradiated samples thanks to ^{98}Mo(n,γ) reaction contributions which occur in an energy range wider than the resonance region. The radionuclide contaminants level inside samples is however worse than the ones available from the TRASCO RFQ based system, because of additional open reaction channels. The specific activity provided with the activator system proposed, driven by 50 MeV proton beams, is estimated to be about 25% better than similar experimental devices developed. The final ^{99}Mo production is however poor. The ^{98}Mo/^{100}Mo-enriched mass required for the irradiated samples are:

- M= ~90 gr ^{98}Mo (or 130 gr ^{100}Mo exploiting n,2n reactions) to get 1 Ci in-target activity (EOB) after 24 hrs irradiation;
- M= ~165 gr ^{98}Mo (or 245 gr ^{100}Mo exploiting n,2n reactions) to get 1 Ci in-target activity (EOB) after 12 hrs irradiation

c. The ^{99}Mo direct production, using proton beams hitting ^{100}Mo-enriched thick samples, would instead be of interest. The yields predicted at reference proton energies are consistent with some experimental tests performed. Even assuming, as preliminary design parameter, a relatively low beam power areal density (500 W/cm^2) on irradiated samples, the ^{99}Mo in-target activity (EOB) expected, as well as the ^{100}Mo sample mass required would be:

- Ep= 40 MeV, I=500 μA — M= 113 gr ^{100}Mo, A= ~ 28 Ci after 24 hrs irradiation;
  M= 113 gr ^{100}Mo, A= ~ 15 Ci after 12 hrs irradiation;
- Ep = 70 MeV, I=500 μA — M= 514 gr ^{100}Mo, A= ~ 93 Ci after 24 hrs irradiation;
  M= 514 gr ^{100}Mo, A= ~ 50 Ci after 12 hrs irradiation.

d. The ^{99m}Tc direct production using protons, on same ^{100}Mo-enriched thick samples, would also be very interesting. A selective ^{99m}Tc production, with a minimum ^{99}Mo yield, would require proton beams up to 25 MeV. Considering the SPES cyclotron minimum output energy (40 MeV), without an energy degrader system coupled, the overall resulting ^{99m}Tc in-target activity after 24 hrs irradiations is comparable to that for ^{99}Mo under 70 MeV beams. Assuming the

same beam power areal density (500 W/cm^2) on sample being irradiated, the ^{99m}Tc in-target activity concentration (EOB) expected, as well as the ^{100}Mo sample mass required would be:

- Ep= 40 MeV, I=500 μA M= 113 gr ^{100}Mo, A= ~ 97 Ci after 24 hrs irradiation;
  M= 113 gr ^{100}Mo, A= ~ 78 Ci after 12 hrs irradiation;

However when proton beam energy is instead 25 MeV for a more specific ^{99m}Tc production the estimated yields are as follows:

- Ep= 25 MeV, I=500 μA M= 30 gr ^{100}Mo, A= ~ 73 Ci after 24 hrs irradiation;
  M= 30 gr ^{100}Mo, A= ~ 58 Ci after 12 hrs irradiation;

In conclusion, the direct proton reaction on ^{100}Mo-enriched targets is by far the preferable way of accelerator-based ^{99}Mo/^{99m}Tc production, providing good activity levels. It has to be outlined that, in case of ^{99m}Tc direct production, the long-lived isomer ^{99g}Tc is also produced at a rate estimated to be at least about a factor three faster. If long irradiations are performed, the ^{99g}Tc thus generated may reach levels for which the N^{99gTc}/N^{99mTc} atomic ratio exceeds 4, which is considered an upper, still acceptable limit for scintigraphic scans with respect to the ^{99g}Tc/^{99m}Tc available from Mo/Tc generators. Production of ^{99m}Tc via this route may be feasible if a series of short time (i.e. $T_{irr} < ½\ T_{1/2}$) irradiations (1.5-2 hrs) are performed.
However, in all the production cases analyzed but for the one which makes use of TRASCO RFQ accelerator, a series of contaminant radionuclide are produced. Among them, in particular, the pure beta emitter ^{90}Sr having long mean life. Although not mentioned in literature, it deserves a more accurate experimental assessment to evaluate the risks.

References

1 **J.R. Zeevaarta, S. Olsenb**, *Recent trends in the concept of specific activity: Impact on radiochemical and radiopharmaceutical producers*, Applied Radiation and Isotopes 64 (2006) 812–814;
2 **M.S. Uddin, M. Hagiwara, F. Tarkanyi, F. Ditroi, M. Baba**, *Experimental Studies on the Proton-induced Activation Reactions of Molybdenum in the Energy Range 22–67 MeV*, Applied Radiation and Isotopes 60 (2004) 911–920;
3 **B. Scholten, R.M. Lambrecht, M. Cogneau, H. Vera Ruiz, S. M. Qaim**, *Excitation functions for the cyclotron production of 99mTc and 99M*, Applied Radiation and Isotopes 51 (1999) 69-80;
4 **S. Takacs, Z. Szucs, F. Tarkanyi, A. Hermanne, M. Sonck**, *Evaluation of proton-induced reactions on ^{100}Mo: New cross sections for the production of ^{99m}Tc and ^{99}Mo*, Journal of Radioanalytical and Nuclear Chemistry, 257, 1, (2003) 195-201;
5 **M.C. Lagunas-Solar, P.M. Kiefer, O.F. Carvacho, C.A. Lagunas Y.P. Chaf**, *Cyclotron Production of NCA 99mTc and 99 Mo. An Alternative Non-reactor Supply Source of Instant 99mTc and 99 Mo + 99mTc Generators*, Applied Radiation and Isotopes 42, 7, (1991) 643-651, International. Journal of Radiation Applications and Instruments Part A;
6 **R.M. Lambrecht, T. Sekineb, H.V. Ruizc**, *Alice predictions on the accelerator production of molybdenum-99*, Applied Radiation and Isotopes 51 (1999) 69-80;
7 IAEA Exfor Nuclear Database;

8 **C. Rubbia,** *Resonance enhanced neutron captures for element activation and waste transmutation* CERN/LHC/97-0040EET, 1997;

9 **TARC collaboration,** *Neutron-driven nuclear transmutation by Adiabatic Resonance Crossing,* CERN-SL-99-036EET, 1999;

10 **C. Rubbia,** *Neutron-Driven Element Transmuter,* PCT/EP97/03218 (1997);

11 **S. Agosteo, P.Colautti, J. Esposito, A. Fazzi, M.V. Introini, A. Pola,** *Characterization of the Energy Distribution of Neutrons Generated by 5 MeV Protons on a Thick Beryllium Target at Different Emission Angles,* Applied Radiation and Isotopes (2011), doi:10.1016/j.apradiso.2011.03.015;

12 **I. Tilquin, P. Froment, M. Cogneau, Th. Delbar, J. Vervier, G. Ryckewaert,** *Experimental measurements of neutron fluxes produced by proton beams (23–80 MeV) on Be and Pb targets,* Nuclear Instruments and Methods A 545 (2005) 339–343;

13 **T. Aoki, M. Baba, S. Yonai, N. kawata, M. Hagiwara, T. Miura, T. Nakamura,** *Measurement of Differential Thick-Target Neutron Yields of C, Al, Ta, W(p,xn) for 50 MeV Protons;* Nuclear Science and Engineering, 146, (2004) 200-208;

14 **P. Froment, I. Tilquin, M. Cogneau, Th. Delbar, J. Vervier, G. Ryckewaert,** *The production of radioisotopes for medical applications by the adiabatic resonance crossing (ARC) technique,* Nuclear Instruments and Methods in Physics Research A, 493, 3, (2002) 165-175;

15 **K.Abbas, S. Buono, N. Burgio, G. Cotogno, N. Gibson, L. Maciocco, G. Mercurio, A. Santagata, F. Simonelli, H. Tagziria,** *Development of an accelerator driven neutron activator for medical radioisotope production,* Nuclear Instruments and Methods in Physics Research A, 601, (2009) 165-175;

16 **J. V. Evans, P. W. Moore, M. E. Shying, J. M. Sodeau,** *Zirconium Molybdate Gel as a Generator for Technetium-99m I. The Concept and its Evaluation,* Applied Radiation and Isotopes 38, 1, (1987) 19-23, International. Journal of Radiation Applications and Instruments Part A;

17 **F.F Knapp, S. Mirzadeh,** *The continuing important role of radionuclide generator systems for nuclear medicine,* European Journal of Nuclear Medicine Vol. 21, No. 10, October 1994;

18 **S. Chattopadhyay, S. Saha Das, M.K. Das, N.C. Goomer,** *Recovery of 99mTc from Na2[99Mo]MoO4 solution obtained from reactor-produced (n,g)^{99}Mo using a tiny Dowex-1 column in tandem with a small alumina column,* Applied Radiation and Isotopes 66 (2008) 1814–1817;

19 **S. Chattopadhyay, S. Saha Das, L. Barua,** *A simple and rapid technique for recovery of 99mTc from low specific activity (n,g)^{99}Mo based on solvent extraction and column chromatography,* Applied Radiation and Isotopes 68 (2010) 1-4;

20 **Y. Nagai Y. Hatsukawa,** *Production of 99Mo for Nuclear Medicine by 100Mo(n,2n)99Mo,* Journal of the Physical Society of Japan, 78, 3, (2009);

21 **C.M. Logan, D.W. Heikkinen,** *RTNS-II - A Fusion Materials Research Tool,* Nuclear Instruments and Methods 200 (1982) 105-111;

22 **D.W. Heikkinen, J.C. Davis, D.J. Massoletti, D.W. Short, D.B. Tuckerman,** *The RTNS-II Fusion Materials Irradiation Facility,* Journal of Nuclear Materials 141-143 (1986) 1061-1063;

23 **X. Ledoux et al.,** *A neutron beam facility at SPIRAL-2,* International Conference on Nuclear Data for Science and Technology 2007, DOI: 10.1051/ndata:07703;

24 **P. Garin,** *IFMIF: Status and developments,* Proc. of EPAC. 2008, Genoa, Italy 974-977;

25 **J. Reijonen, F. Gicquel, S.K. Hahto, M. King, T.-P. Lou, K.-N. Leung,** *D–D neutron generator development at LBNL,* Applied Radiation and Isotopes 63 (2005) 757–763;

26 **N. Levkovskii,** *Middle Mass Nuclides (A=40±100) Activation Cross Sections by Medium Energy (E=10±50 MeV) Protons and a-Particles (Experiment and Systematics),* Inter-Vesti, Moscow, (1991) 215;

27 **B. Guerin S. Tremblay, S. Rodrigue, J. A. Rousseau, V. Dumulon-Perreault, R. Lecomte, J. E. van Lier, A. Zyuzin, E. J. van Lier,** *Cyclotron Production of 99mTc: An Approach to the Medical Isotope Crisis,* The Journal of Nuclear Medicine, Vol. 51(4), 2010;

28 **H. Targholizadeh, G. Raisali, A.R. Jalilian, M. Ensaf, M.K. Dehghan, N. Rostampour,** *Cyclotron production of technetium radionuclides using a natural metallic molybdenum thick target and consequent preparation of [Tc]-BRIDA as a radio-labeled kit sample,* Nukleonica 55(1) (2010) 113-118;

29 **P. Möller, J. R. Nix, W. D. Myers, and W. J. Swiatecki**, Atomic Data Nucl. Data Tables 59, 185-381 (1995);

30 **A.J. Koning and D. Rochman,** TENDL-2009: "TALYS-based Evaluated Nuclear Data Library", Nuclear Research and Consultancy Group (NRG) Petten, The Netherlands, (2009) http://www.talys.eu/tendl-2009;

31 **European Commission, Health and Consumers Directorate General,** *Preliminary report on supply of radioisotopes for medical use and current developments in nuclear medicine,* SANCO/C/3/HW D(2009) Rev. 8, Luxembourg, 30 Oct. 2009);

32 **A. Pisent, M. Comunian, A. Palmieri, E. Fagotti, G.V. Lamanna, S. Mathot,** *The TRASCO SPES-RFQ.* Proceedings of LINAC 04 Conference, Lubeck, Germany, 2004, 69-71;

33 **E. Fagotti, M. Comunian, A. Palmieri, A. Pisent, C. Roncolato, F. Grespan,** *Fabrication and Testing of TRASCO,* Proceedings of LINAC 08, Victoria BC, Canada, 2008, 151-153;

34 **C. Ceballos, J. Esposito,** *The BSA modeling for the accelerator-based BNCT facility at INFN LNL for treating shallow skin melanoma,* Applied Radiation and Isotopes 67 (2009) S274-S277;

35 **J. Esposito, P. Colautti, S. Fabritsiev, A. Gervash , R. Giniyatulin, V.N. Lomasov, A. Makhankov, Mazul, A. Pisent, A. Pokrovsky M. Rumyantsev, V. Tanchuk, L. Tecchio,** *Be target development for the accelerator-based SPES-BNCT facilityat INFN Legnaro,* Applied Radiation and Isotopes 67 (2009) S270-S273;

36 **G. Prete** Edt, *SPES advanced exotic ion beam facility at LNL.* Technical Design Report, (2008) INFN-LNL-223;

37 **NIST Physical laboratory,** STAR database http://www.nist.gov/pml/data/star/index.cfm;

38 **International Commission on Radiation Units and Measurements.** *ICRU Report 37, Stopping Powers for Electrons and Positrons* (1984);

39 **International Commission on Radiation Units and Measurements.** *ICRU Report 49, Stopping Powers and Ranges for Protons and Alpha Particles* (1993);

40 **B. Scholten et al.,** *Data file EXFOR-O0737.002 dated 1989,* compare Applied Radiation and Isotopes 51,69, (1999). EXFOR data retrieved from the IAEA Nuclear Data Section (NDS), Vienna;

41 **B. Scholten et al.,** *Data file EXFOR-O0737.003 dated 1989, compare* Applied Radiation and Isotopes 51,69, (1999). EXFOR data retrieved from the IAEA Nuclear Data Section (NDS), Vienna;

42 **S. Takacs et. al.,** *Data file EXFOR-D4115.002.2 dated 2003, compare* Journal of Radioanalytical and Nuclear Chemistry. 257,1,(2003). EXFOR data retrieved from the IAEA Nuclear Data Section (NDS), Vienna;